N-79234

PROGRESS REPORT NO. 30-4

# THE EFFECT OF RAPID LIQUID-PHASE REACTIONS ON INJECTOR DESIGN AND COMBUSTION IN ROCKET MOTORS

GERARD W. ELVERUM, JR.
PETER STAUDHAMMER



JET PROPULSION LABORATORY
CALIFORNIA INSTITUTE OF TECHNOLOGY
PASADENA, CALIFORNIA
AUGUST 25, 1959

National Aeronautics and Space Administration
Contract No. NASw-6

PROGRESS REPORT No. 30-4

# THE EFFECT OF RAPID LIQUID-PHASE REACTIONS ON INJECTOR DESIGN AND COMBUSTION IN ROCKET MOTORS

Gerard W. Elverum, Jr.
Peter Staudhammer

Donald R. Bartz

Donald R. Bartz, *Chief*
*Power Plant Research Section*

Copy No.__________

JET PROPULSION LABORATORY
California Institute of Technology
Pasadena, California
August 25, 1959

## CONTENTS



## TABLES

**Page intentionally left blank**

## FIGURES

## COLOR PLATES

## COLOR PLATES (Cont'd)

Page

## ABSTRACT

Data are presented indicating the rates and magnitudes of energy released by the liquid-phase reactions of various propellant combinations. The data show that this energy release can contribute significantly to the rate of vaporization of the incoming propellants and thus aid the combustion process. Nevertheless, very low performances were obtained in rocket motors with conventional impinging-jet injectors when highly reactive systems such as $N_2O_4$–$N_2H_4$ were employed. A possible explanation for this low performance is that the initial reactions of such systems are so rapid that liquid-phase mixing is inhibited. Evidence for such an effect is presented in a series of color photographs of open flames using various injector elements.

Based on these studies, some requirements are suggested for injector elements using highly reactive propellants. Experimental results are presented of motor tests using injector elements in which some of these requirements are met through the use of a set of concentric tubes. These tests, carried out at thrust levels of 40 to 800 lb per element, demonstrated combustion efficiencies of up to 98% based on equilibrium characteristic velocity values. Results are also presented for tests made with impinging-jet and splash-plate injectors for comparison.

## I. INTRODUCTION

Several years ago, stabilized fuming nitric acid, SFNA ($HNO_3$ containing 14 wt % $NO_2$, 2 to 3 wt % $H_2O$, and 0.5 wt % HF), was substituted in the *Corporal* rocket engine for red fuming nitric acid, RFNA ($HNO_3$ containing 6.8 wt % $NO_2$). This change in oxidizer composition caused unstable combustion and a large loss of performance with the aniline-based fuel used. Because of these unexpected results, an experimental investigation was carried out to determine the influence of water and $NO_2$ on the combustion process in the nitric acid–aniline plus furfuryl alcohol propellant system. The detailed findings of this study are reported in Ref. 1, the conclusions of which are summarized below:

1. The axial energy-release profile within a combustion chamber is controlled primarily by the rate of mixing and vaporization of the incoming liquids and the rate at which the vapors are superheated to their ignition temperature.

2. The rate of vaporization of certain liquid propellants mixed in a manner which produces droplets composed of both fuel and oxidizer can be controlled by the rate of energy released by liquid-phase and liquid-vapor reactions within the mixed droplets.
3. The amount of energy released by the liquid-phase reactions is determined by the rate and microscale of mixing prior to film breakup and droplet evaporation. The extent of molecular mixing controls directly the amount of energy supplied by neutralization and other reactions having very small activation energies.
4. Additional energy release in the liquid phase can be controlled by the presence of certain catalytic species necessary for the rapid utilization by nitration (or oxidation) of the energy made available by neutralization (or reactions of near-zero activation energy).

Studies of the kinetics and mechanisms of aromatic hydrocarbon nitrations show that the nitronium ion $NO_2^+$, known to be present in anhydrous acid, plays a major catalytic role. Electrical conductance measurements indicate that about 5% water is sufficient to suppress the self-ionization of nitric acid almost completely. Therefore, the large change in performance and in ignition delay of the acid–aniline systems resulting from the addition of a relatively small amount of water to the acid may have been the result of a significant decrease in nitration rate in the liquid phase which greatly reduced the vaporization rate and the superheat temperature of the propellants.

Because this work indicated that the liquid-phase reactions may be very important in determining the overall combustion delay and, therefore, both the combustion efficiency and stability in nitric acid oxidized systems, a program was undertaken at the Jet Propulsion Laboratory to investigate the thermal behavior and the injector design requirements of liquid-phase-reactive propellant systems.[1]

[1]The authors wish to gratefully acknowledge the valuable contribution of guidance and assistance made by Arthur F. Grant, Jr., in his supervision of the program.

# II. RATES AND MAGNITUDES OF LIQUID-PHASE REACTIONS

Measurements by other investigators of rates of temperature rise in various types of stirred reactors have shown that times of thermocouple response and mixing rates in such reactors limited the minimum reaction times which could be measured to the order of tenths of a second. Since we were interested in times of the order of a few milliseconds and also wished to study reactions under high pressure, a concentric-tube flow system was built with a retractable inner tube. A schematic diagram of this apparatus is shown in Fig. 1. Another configuration of the center tube that was used for some of the tests ended in a sharp knife edge at its downstream end (see Fig. 2), rather than the blocked end and radial holes shown in Fig. 1.

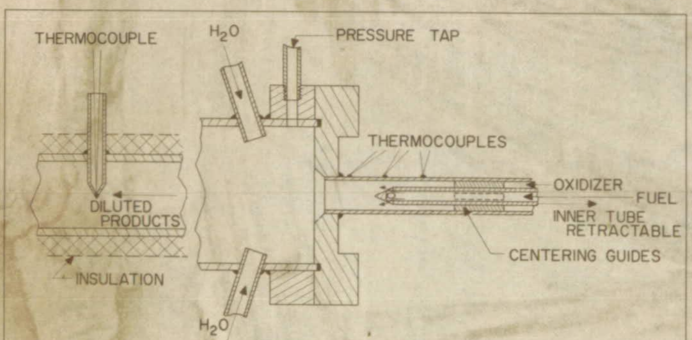


**Fig. 1. Mixing, Pressurizing, and Dilution Regions of the Liquid-Phase Reactor**

The mixing characteristics for several inner-tube designs were studied utilizing the neutralization reaction between dilute KOH and $HNO_3$. In Fig. 2 the percentage of neutralization is plotted vs mixing length in tube diameters. The percentage was obtained by dividing the temperature rise read on the tube thermocouples by the temperature rise as measured for the same fluids in an adiabatic calorimeter. It can be seen that the tube thermocouples give quite an accurate result for the total temperature rise. The mixing rate of the knife-edge tube depends on turbulent diffusion and is quite sensitive to mixture ratio, whereas the four-hole-tube designs gave over 90% of complete molecular-scale mixing in 5 diameters (in about 1 millisec). Also, the four-hole-tube mixing rate is nearly independent of mixture ratio, at least up to ratios of 3. The fluid velocities were of the order of 40 ft/sec, and the time scale is based on a density of 1.0.

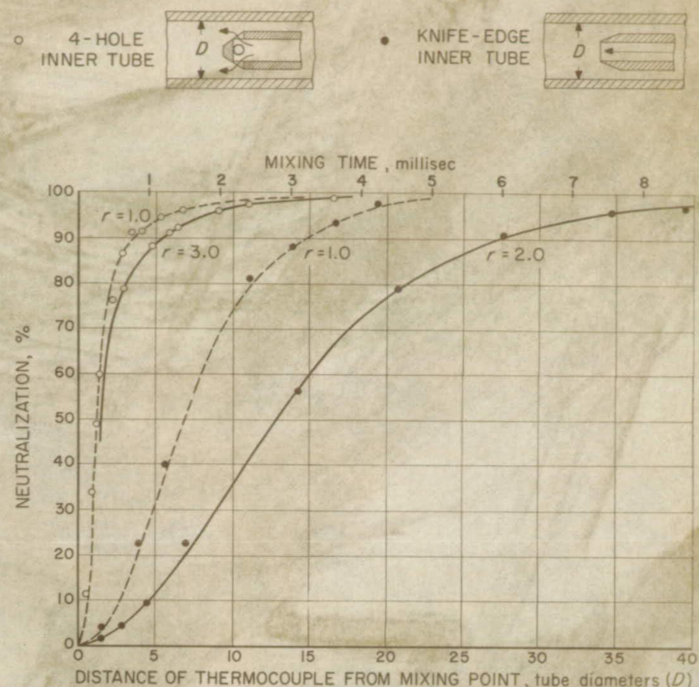


**Fig. 2. Mixing Characteristics for Two Types of Inner Tube**

Measurements of a series of aliphatic alcohols were made in order to determine the effect of chain length and branching on the initial reactions with acid. Results of these tests are shown in Fig. 3. The initial profile of temperature rise vs mixing length can be seen to follow the mixing-rate curve (Fig. 2) for the apparatus. The reaction responsible for most of the temperature rise is probably a simple weak neutralization of the fuel. Approximate calculations indicate about 3 kcal/mole for each alcohol. However, in the case of isopropyl alcohol, a second reaction is activated.

Tests were also made with diisobutylene in JP4 and hydrazine in isopropyl alcohol to test the ability of the apparatus to determine the effect of additives. Isopropyl alcohol had tended to give unstable combustion with acid in several motors operated at the Laboratory. Addition of 5–10% hydrazine had resulted in smooth combustion over a wide range of mixture ratios. The data show an increase in temperature at a rate equal to the mixing rate up to the maximum temperature. If the nitration reaction then occurs, it must result in vaporization and can not be detected by temperature rise.

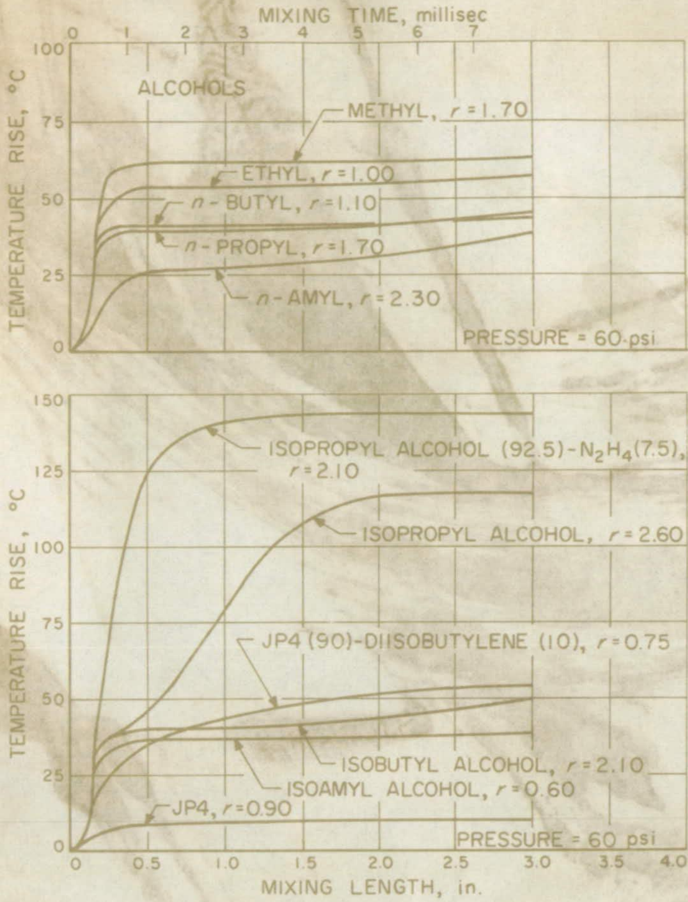


**Fig. 3. Temperature Rise vs Mixing Time for SFNA with Indicated Fuels**

Because the addition of additives to JP4 had resulted in improved stability with acid in several motors as reported by Aerojet,[2] Reaction Motors,[3] and others, a series of tests was carried out with various additives to JP4 to determine if part of the reason for this improvement could be found in the initial reaction rates in the liquid phase.

The effects of UDMH and several other reactive additives are shown in Fig. 4. The effect of pressure on the maximum temperatures attained, and the fact that doubling the concentration of UDMH does not result in a doubling of the temperature rise, indicate that the values of the maximum temperatures above about 5% UDMH may be limited by vaporization of the resultant mixture. The temperatures attained by a mixture of methyl alcohol and diethylenetriamine, which is one of the most energetic nonhypergolic systems studied, is also shown in Fig. 4 for purposes of comparison.

The temperature rise as a function of mixture ratio after complete mixing is shown in Fig. 5. The fact that the maxima occur at very low mixture ratios indicates that liquid-phase reactions probably occur primarily between the acid and the additive, so that the quantity of acid required is low compared to total fuel weight. Figure 5 also shows that systems in which the main fuel

[2] Aerojet-General Corp., Azusa, Calif.

[3] Reaction Motors, Inc., Denville, N. J.

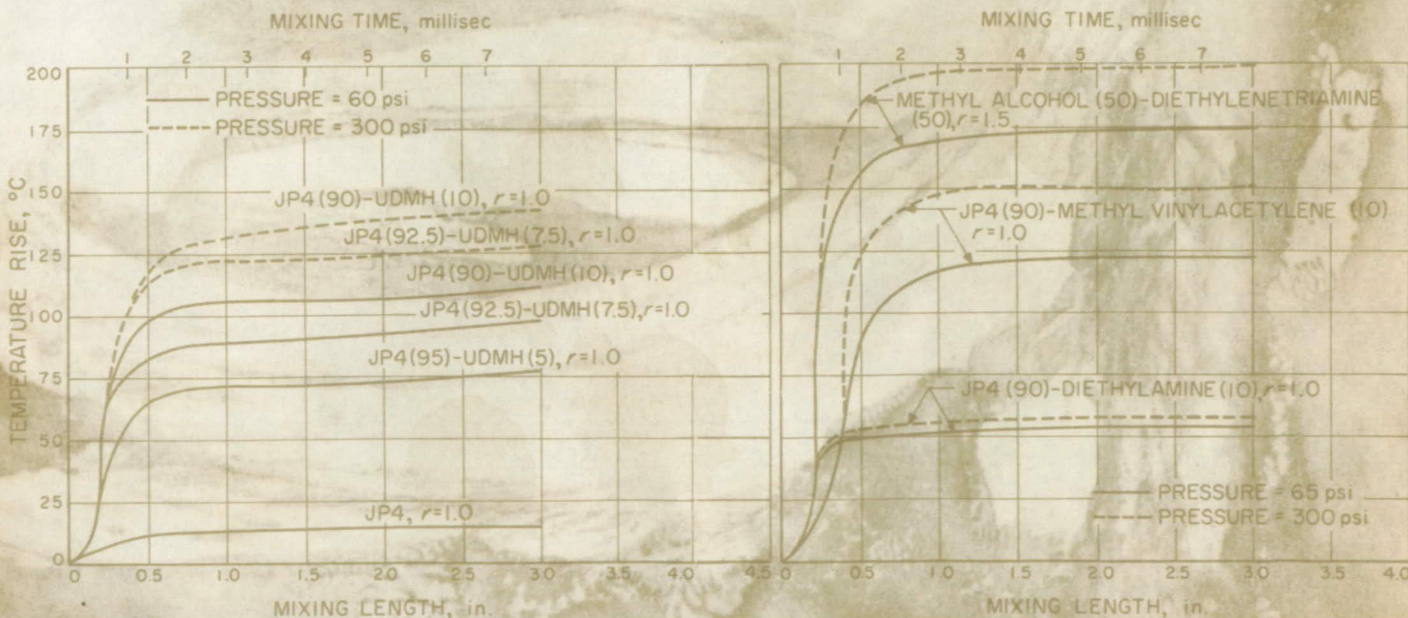


**Fig. 4. Rates of Temperature Rise for Reactions of Various Fuels with SFNA**

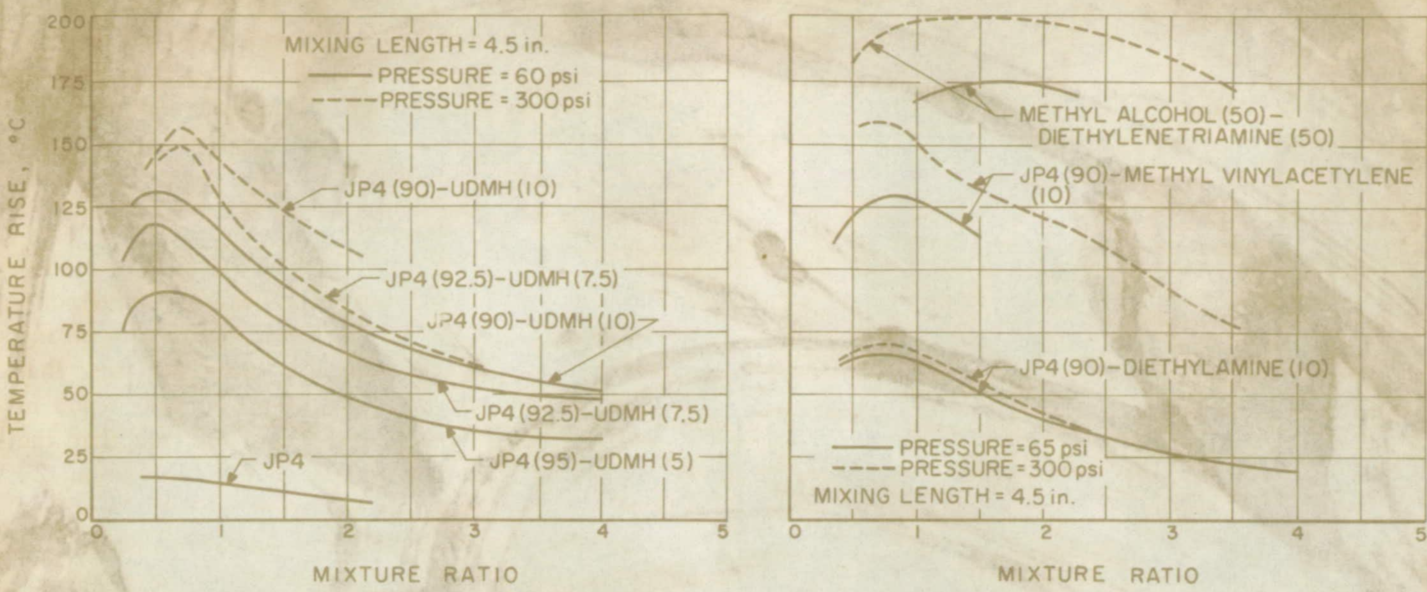


**Fig. 5. Values of Maximum Temperature Rise for Reactions of Various Fuels with SFNA as a Function of Mixture Ratio**

component may undergo fast liquid-phase reactions at several positions in the molecule have considerable self-vaporization, even at their respective mixture ratios for optimum combustion. (See the curve for methyl alcohol plus diethylenetriamine.) Fuels such as JP4 which do not undergo any appreciable fast reactions with SFNA in the liquid phase will generally have widely different mixture ratios for maximum performance than for maximum temperature rise when relatively small amounts of additives are used. Optimum additives, therefore, should have a high ratio of reactive centers to molecular weight.

An approximate calculation of the heat of reaction per mole of UDMH required to raise the mixture reaction temperature from that of pure JP4–acid to that indicated for 10% UDMH in JP4 at 60 psi, assuming no vaporization and a mixture heat capacity of 0.5, gives a heat reaction of about 75 kcal per mole of UDMH. At 300 psi, assuming no vaporization, a value of about 90 kcal per mole of UDMH is indicated. This energy is sufficient to completely vaporize the SFNA–UDMH propellant system at a mixture ratio of 2.5 and to superheat the vapors to very high temperatures.

An approximate calculation of the heat of reaction per mole of the diethylamine gives 35 kcal per mole of fuel, which could be the result of a single anhydrous neutralization or nitration. However, a calculation for methyl vinylacetylene at 300 psi, assuming no vaporization, gives about 105 kcal/mole. It seems apparent that nitration reactions at unsaturated bonds must occur with a rapidity only slightly less than the rate of mixing, and that this fuel molecule must undergo several energetic reactions. It is probable that some actual oxidation is occurring, because the value of 105 kcal per mole of fuel is over one-quarter of the total heat expected for complete combustion of this fuel. A calculation of the heat released per average mole of JP4 alone ($MW \simeq 184$) gives only 2.4 kcal/mole or about 13 cal/gm, and it therefore seems quite clear that only vapor-phase reactions of this material are of any importance.

The approximate calculations of heat release per mole of additive to the relatively inert solvent JP4 when oxidized by SFNA show that about 90 kcal/mole is released by UDMH and about 105 kcal/mole is produced by methyl vinylacetylene. Since it is assumed that no heat went into vaporization at the high liquid temperatures involved, these values should be conservative estimates. Their magnitude indicates that liquid-phase reactions can indeed be very energetic. Furthermore, the reactions occur in times of the order of the mixing time of the propellants.

# III. MIXTURE-RATIO DISTRIBUTION AND COMBUSTION EFFICIENCY

From the foregoing sections it can be concluded that the best injector design for hypergolic propellant combinations is one which will produce maximum liquid-phase mixing. While the liquid-phase reactions will then control the vaporization rate and accelerate the combustion process, the over-all combustion efficiency attained in any given chamber is also dependent on the uniformity of the mixture-ratio distribution produced by the injector.

Most engines are operated at over-all mixture ratios corresponding to the maximum on a theoretical performance curve. Since any deviation from this mixture ratio therefore results in lower performance, it is apparent that not only the over-all but the local mixture ratios, as well, must be accurately controlled if highest performance is to be attained. Combustion may be kinetically complete in relatively short distances over a wide range of mixture ratios for any particular propellant combination. However, at any over-all mixture ratio near maximum performance, the sum of the energy released by complete combustion of propellants operating at various local mixture ratios in the chamber will always be less than that produced by having all local mixture ratios equal to the over-all ratio. Any deviations in local mixture ratio produced by an injector element can only be corrected by turbulent mixing and diffusion in a relatively low density accelerating fluid. Such a process in normal chamber geometries requires fairly long chamber lengths proportional to the size of the nonuniform local mixture-ratio regions. Therefore, unless a very large number of injector elements are used, the resulting mixture-ratio distribution produced by each element should be as uniform as possible.

Injector types such as the showerhead or like-on-like patterns produce mixture-ratio distributions which vary greatly from point to point and utilize little of the available liquid-phase reaction energy for vaporization. The use of impinging streams of oxidizer on fuel in the case of the acid-oxidized propellant systems produced the best performance in the smallest chamber of element types except a premixer. For example, a double row of impinging doublets was used with success in the injector of the *Corporal* engine and in the second-stage *Vanguard* engine.

Some tests conducted during this program using dilute acid and base solutions, as well as previous investigations using dyed inert liquids (Ref. 2), have shown that the individual droplets in the spray resulting from impinging streams actually contain both propellants at a mixture ratio close to the local-spray mixture ratio. The present test measurements determined the $pH$ of the droplets of a spray sample by impinging them on special indicator paper. Thus, impinging the propellants (providing they are not too reactive, as will be pointed out later) will provide good liquid-phase mixing down to the sub-droplet scale.

It is not sufficient, however, to merely obtain geometrical alignment of impinging streams if a uniform local mixture-ratio distribution is to be obtained. Work carried out at the Laboratory (Ref. 3) has shown that the velocity profile of the streams must be symmetrical and that the momentum ratio for a pair of impinging streams must have a singular value for any particular propellant combination at any given mixture ratio to give most uniform mixture-ratio distribution. In Ref. 4, equations relating the optimum mixture-ratio distribution to the mixture ratio, orifice-area ratio, and propellant-density ratio were given for several other impinging-stream elements. Those elements covered were a two-on-one, a two-on-two, and a four-on-one.

The importance of operating at the correct mixture ratio for a given orifice-area ratio can be seen from Plates 1 and 2. Plate 1 shows an open-flame test of two SFNA streams impinging on one JPX stream. The operating mixture ratio in this case does not meet the momentum-ratio requirements for uniform mixture-ratio distribution specified in Ref. 4 for a triplet injector element. The fuel stream does not penetrate the oxidizer, but is deflected to the outside of the spray fan. The central 90 deg of the spray which is rust colored is so oxidizer rich that ignition does not even occur. At the edges of this oxidizer-rich region are two narrow zones where the oxidizer and fuel are well enough mixed that a bipropellant flame is established. These regions appear as a hot blue flame in Plate 1. At the outer edges of the spray, the fuel-rich droplets ignited by the bipropellant flame burn with the surrounding air. The white patch obscuring part of the bipropellant flame area at the bottom of the spray is caused by fuel vapor burning in air outside the plane of the spray.

The same injector element is shown in Plate 2 operating near the fluid-velocity ratio which is optimum for producing good mixture-ratio distribution. In this case a hot flame is produced throughout most of the spray except at the very outer edges where some fuel-rich vapor is mixing and burning with air. It is apparent that mere spatial alignment of impinging streams is not satisfactory if good combustion efficiency is to be produced.

The two photographs show an additional feature of interest. In Plate 1, the center of the spray near the impingement point appears dark because only nearly pure liquid oxidizer exists in the fluid film in this region. The two areas on either side show an indication of liquid reaction causing vaporization and evolution of $NO_2$. The extreme outer edge of the initial spray shows less vapor. Farther out in the spray, in line with the area of $NO_2$ evolution, are the regions of spontaneous ignition and bipropellant combustion. In Plate 2, the uniformity of vapor and $NO_2$ gas is quite apparent near the impingement point. The effect of these two distributions on the combustion efficiency expected in a rocket engine is quite obvious.

# IV. THE EFFECT OF LIQUID-PHASE REACTIONS ON VAPORIZATION AND COMBUSTION RATES

An injector element composed of two oxidizer streams impinging on two fuel streams is shown in Plate 3 operating with SFNA and JPX. This propellant system produces just enough heat to be hypergolic under certain conditions. The element is shown operating near the optimum mixture-ratio distribution condition. Neglecting the tenuous yellow-toned vapor-air flame, the main spray shows a relatively uniform bipropellant combustion zone occurring several inches away from the point of impingement. The structure of the spray shows a narrow cone angle which is very similar to that produced by this element with inert fluids. Although some vapor evolution is evident, its rate and magnitude do not significantly affect the remaining liquid-spray mass distribution. A large number of liquid-droplet streaks can be seen, each droplet finally bursting into flame.

A large amount of products from the initial reactions are condensed against the cool face of the injector. This material is primarily the result of the back spray which amounts to about 10% of the total flow for this type of element. The cooling is sufficient to prevent ignition, and the material simply foams off the face of the injector as gases are generated within the liquid mass.

The more reactive system SFNA–UDMH with the same type of injector is shown in Plate 4. Practically no ignition delay is apparent, and the absence of liquid-drop streaks indicates a more rapid vaporization. Although the back-spray products condense on the cool injector face, the surface of this foam is ignited and burns. The products closest to the injector face are apparently cooled below the ignition temperature and flow downward off the injector flange. The resulting mass distribution in the main spray shows some expansion over the water spray pattern. The small increase in cone angle, however, indicates that although ignition of the initial vapors is almost instantaneous, the main vapor evolution probably occurs sometime after liquid film breakup into droplets.

Three different mixture ratios of the propellant combination $N_2O_4$–UDMH are shown in Plates 5, 6, and 7. Plate 5 shows operation at a mixture ratio more fuel rich than the ratio for optimum mixing. The rapid evolution of gas at the impingement point has greatly increased the resultant spray-cone angle. The spray is fuel rich on the outside, as indicated by the streak patterns of a few fuel droplets. The wide angles of divergence of these streaks indicate that initial vapor generation occurred violently within the initial liquid mass just after impingement. This gas evolution is apparent in the photographs. There is only a trace of condensed froth on the injector face, and the light liquid film that does cover the face from the direct back spray burns immediately without dripping off. Apparently, unlike the acid-oxidized systems, the $N_2O_4$ system does not form high-boiling, fairly stable liquid products. It is probable that some direct oxidation to water vapor and other gases occurs.

In Plates 6 and 7, operation is shown at oxidizer-rich and optimum mixture ratios, respectively. Nearly complete self-vaporization is indicated.

Thus, by utilizing hydraulically stabilized impinging streams (as defined by the criteria of Ref. 3) with the correct velocity ratio for optimum mixing, a uniform, self-vaporizing propellant mixture can be developed by each injector element for most hypergolic systems. Injector elements producing uniform primary mixing with hypergols can eliminate much of the critical dependence of combustion efficiency on recirculation patterns normally required to supply both heat for vaporization and ignition, and turbulence for secondary mixing.

# V. RESULTS FOR EXTREMELY REACTIVE PROPELLANT SYSTEMS

As a result of system studies made early in 1957, the Laboratory undertook the investigation of two promising storable propellant combinations: $N_2O_4$–hydrazine and $ClF_3$–hydrazine. Based on the results described above, the injector supporting-research program proposed for these storable systems had the following objectives:

1. Development of an injector element which would produce as uniform a mixture-ratio distribution as possible.
2. Determination of the scaling characteristics of such an element up to 5,000-lb thrust, so that the minimum number of elements required for any total-thrust level and chamber geometry could be specified.
3. Investigation of the effect of various combinations of such elements on the combustion profile and stability at several total-thrust levels.

Initial testing of these two hypergolic combinations was carried out using impinging-stream single-injector elements at various thrust levels. Tests were also made at JPL's Edwards Air Force Base Test Station using a double row of impinging streams at 20,000-lb thrust with orifices modified to meet the optimum mixing criteria for $N_2O_4$ and $N_2H_4$. The performance results from these early tests were disappointingly low. In one type of 20,000-lb injector having 90 pairs of impinging streams, a characteristic velocity of only 4,100 ft/sec was obtained. In addition, extremely rough combustion occurred in most cases. Using single-element configurations such as doublets and triplets, which worked well with acid-oxidized hypergolic systems using fuels other than hydrazine, performance was low and, in addition, explosions occurred throughout each of the tests with $N_2O_4$ and $N_2H_4$.

The two-on-two element gave the highest performance and stability with both $N_2O_4$–$N_2H_4$ and $ClF_3$–$N_2H_4$, but the maximum characteristic velocity at 500-lb thrust was still only 5,300 ft/sec. To find the reasons for this low performance, studies were made of open flames of $N_2O_4$–$N_2H_4$ and of the combustion of $N_2O_4$–$N_2H_4$ in transparent rocket-motor chambers. From these studies it appeared that the low performance obtained with $N_2O_4$–$N_2H_4$ resulted because these liquids react so rapidly that normal liquid-phase mixing and distribution does not have time to occur. The impingement of a stable liquid stream of $N_2O_4$ on a stream of $N_2H_4$ appears to result in an immediate violent vapor evolution at the interface of the two liquids. Thus, a substantial portion of the oxidizer and fuel may be blown apart without being mixed. Furthermore, the violence of the effect disturbs the incoming streams so that the mixing and reaction which does occur is highly unstable.

The impingement of concentric streams of water on the flat end of a rod is shown in Plate 8. A thin, slightly cone-shaped fan is formed. The same concentric set of tubes having $N_2O_4$ flowing through the outer annulus and $N_2H_4$ through the inner tube is shown in Plate 9. The dark reddish region on the right and the yellowish region on the left suggest that the oxidizer and fuel were separated by the violence of the initial reaction before mixing could take place. The $N_2O_4$ appears to undergo a reversal of direction, while the $N_2H_4$ is forced forward into a narrow cone around the rod where it burns with air, producing a characteristic yellowish flame. A hot flame exists between these two zones where some mixing has occurred. The contrast in mass distribution between Plates 8 and 9 is very striking.

The impingement at 180 deg of a stream of $N_2O_4$ on a stream of $N_2H_4$ is shown in Plate 10. The separation of fuel and oxidizer is again suggested by the dominantly reddish zone on the left. In Plates 11 and 12 impingement is shown at 120 and 45 deg, respectively. In Plate 11, streaks from hydrazine droplets can be seen moving even at right angles to the resultant spray fan, which would be quite flat if the fluids were inert. The yellowish region is characteristic of $N_2H_4$-rich combustion with air.

Plate 13 shows two frames from a high-speed motion picture of a single pair of impinging streams designed on the basis of equal stream momentum (Ref. 3) operating in a transparent combustion chamber at 200 psia. Again, evidence of incomplete mixing of fuel and oxidizer, even at high pressure, is shown. In Plate 14, two sequences of frames from this motion picture show that the hydrazine-rich vapor region undergoes violent explosions about 100 times a second. Thus, the low performance obtained with impinging-stream injectors may be due to very poor initial mixture-ratio distribution, persisting even out through the nozzle.

It had been found in a series of small-scale tests carried out at the Laboratory many years ago that a splash-plate injector gave by far the best performance with $N_2O_4$–$N_2H_4$. The reason for this result, in light of the data above, now appears clearer. A schematic injector is shown in Plate 15. On the right side, a typical cross section of a doublet impinging-stream injector is shown. The separation of oxidizer and fuel from the impingement point is indicated. The left-hand side shows a cross section of the same injector with a splash plate in position. The separated oxidizer vapor and spray cannot channel down the wall but are forced past the injector face and pass again into the fuel spray and vapor coming off the lip of the plate. This secondary mixing, plus the flame-anchoring effect of the forced recirculation of hot combustion products, results in a very large increase in performance. Data for impinging-stream injectors are plotted in Fig. 6, both with and without a splash plate, for 20,000- and 45,000-lb thrust.

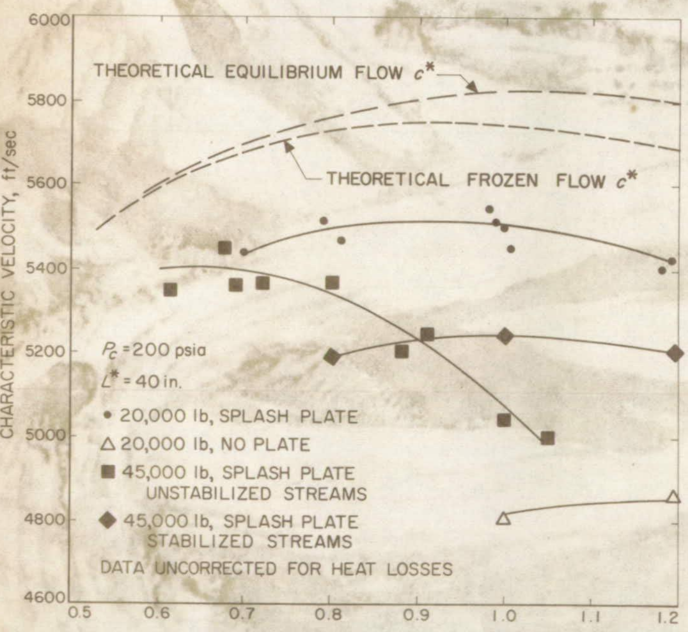


**Fig. 6. Performance of $N_2O_4$–$N_2H_4$ at 20,000- and 45,000-lb Thrust**

Because of the successful results obtained with a splash plate in the 20,000-lb-thrust motor, a splash-plate injector is being investigated for the 5,000-lb-thrust $N_2O_4$–$N_2H_4$ ~~propulsion system presently under development at the Laboratory~~. The results obtained to date with two models of splash-plate injectors for the ~~6,000~~ 5,000-lb motor are shown in Fig. 7. A comparison of these data with the results shown in Fig. 6 indicates that the splash-plate design appears to give lower performance at the higher thrust levels. This result may be connected with the linear dimensions of the larger motors, so that secondary mixing uniformity may be more difficult to achieve. The hydrazine leaving the lip of the plate must travel farther to reach the central oxidizer core. Since the pressure drop across the splash plate indicates a high-velocity compressible fluid flowing out through the splash-plate opening, radial penetration of the hydrazine into this oxidizer-rich flow to give complete secondary mixing may be quite scale limited.

Because of this possible scale limitation and the large $L^*$ required, the splash-plate injector is considered to be only an interim solution for immediate development programs using $N_2H_4$. Work is therefore continuing on the development of stable, high-performance injector elements for extremely reactive systems. Such elements would offer a range of engine scalability and flexibility of operating conditions much wider than is possible with the splash-plate design.

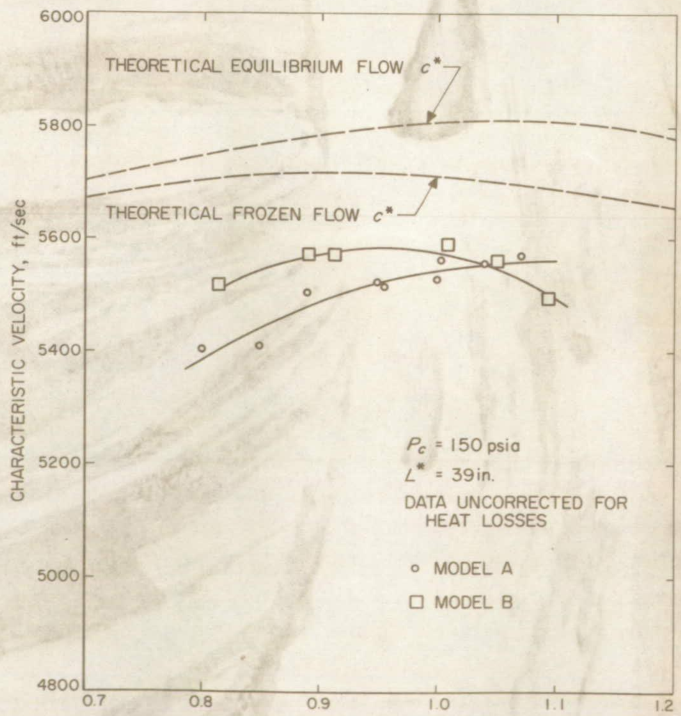


**Fig. 7. Performance of $N_2O_4$–$N_2H_4$ at 6,000-lb Thrust**

level with N2O4–N2H4 propellants. ~~The results~~

# VI. THE CONCENTRIC-TUBE INJECTOR ELEMENT

## A. General Characteristics with Acid-Oxidized Propellant Combinations

One approach to the design of an injector element providing better mixing and higher performance with the $N_2O_4$– and $ClF_3$–hydrazine systems has evolved from the apparatus described in Section II. Designed to study the rates of liquid-phase reactions between fuels and oxidizers, this apparatus consisted of a set of concentric tubes. The inner tube contained radial holes and was retractable so that various amounts of premixing could be obtained. During the studies of liquid reactions, visual observation of the jet issuing from this set of tubes with some premixing showed that for reactive combinations the propellants were extensively vaporized and expanded rapidly and uniformly without any additional atomization technique being required. It appeared that such a device would introduce the propellants into the combustion zone with a uniform mixture ratio and mass distribution.

The water stream emanating from a set of concentric tubes is shown in Plate 16. The end of the inner tube is cut to a knife edge in order to avoid stagnant regions at the end of this tube. The two streams remain concentric and do not diverge even if the stream velocities are unequal. The resultant stream is also unaffected by the retraction of the inner tube into the outer one. As shown in Fig. 2, for nonreactive fluids about 40 diameters of tube length is required for complete mixing at a mixture ratio of 2.0.

The behavior of the streams is quite different with reactive fluids. Plate 17 shows the behavior of the concentric-tube injector with JPX in the inner tube and SFNA in the annulus. The 40 wt % UDMH contained in JPX is just enough to make this propellant combination hypergolic at 1 atmosphere. The inner tube is retracted 0.27 in., which is equivalent to about 4 tube diameters of mixing length (referred to the inside diameter of the outer tube). With inert fluids this amount of retraction produces very little liquid-phase mixing. In Plate 17, the rust color represents regions rich in nitric acid, the bright streaks represent droplets burning, and the bluish flow represents oxidizer-rich gas-phase reaction. The droplets do not burst into flame until enough heat has been generated by liquid-phase reactions to bring the droplets to the ignition temperature. The primary luminous flame is therefore located some distance off the end of the tube. From the picture it is apparent that even at such a small amount of retraction, sufficient mixing and reaction take place to vaporize most of the propellant. Therefore, the mechanism of liquid-phase mixing with these reactive fluids must be very different from that with nonreactive fluids. Apparently the vapors generated upon initial contact break up the individual liquid streams sufficiently to enhance mixing. The resultant premixed vapor-liquid mixture appears to be fairly uniform in mixing-ratio distribution and undergoes smooth combustion.

The characteristics of the flame produced by the concentric-tube injector with the SFNA–JPX propellant system are strongly affected by the extent of retraction. As the inner tube is retracted, the liquid-phase mixing and the extent of the initial reactions are greatly enhanced. At a sufficiently large retraction—about 5 diameters for this system—enough reaction takes place to raise the pressure in the mixing region above the value required for critical flow. The gas-liquid mixture escaping from the outer tube then goes through a shock wave which, it is suggested, atomizes the liquid and further mixes it with the vapors. Subsequent expansion cools the mixture to a temperature sufficiently low to preclude spontaneous ignition.

Plate 18 shows the operation of the SFNA–JPX system described above with a retraction equivalent to 5 diameters (0.35 in.). The gases escaping from the outer tube form an expansion cone characteristic of gases escaping at supercritical pressure. The gaseous products formed upon the initial reactions and cooled by the subsequent expansion are apparently stable enough that they cannot undergo further combustion without the addition of heat from an external source, such as a previously established flame front. The flame is established through spontaneous ignition during the startup transient when the propellant flows have not yet reached their full values and when the vapors escaping from the mixing region have not yet reached sonic flow. The flame front then locates itself at a position where the space velocity of the premixed vapors is equal to the flame-propagation velocity. The uniformity of the flame front gives an indication of the uniformity of mixture-ratio distribution within the vapor. The few random bright streaks in the flame are probably due to mixing and combustion with air.

At retractions greater than 5 diameters the gross characteristics of the vapor generated and the flame do not appear to be different from those shown in Plate 18. Experiments have been carried out with retractions as large as 50 diameters. The pressure generated in the mixing zone and the quantity of gaseous products generated increase with increased retractions, which results in an increase in vapor velocity. Under some conditions the luminous flame can actually be blown out. The vapor generation and, thus, the subsequent combustion were smooth and stable at all retractions below the blowoff limit.

A propellant system slightly more reactive than the SFNA–JPX system is SFNA–UDMH. Plate 19 shows the operation of this system with UDMH in the inner tube at zero retraction. The initial reactions between the two propellants proceed with a very slight ignition delay to produce a mixed vapor which results in a smoothly burning flame. Retraction of the inner tube with this propellant system produces combustion similar to that shown in Plate 18. The two propellants again are premixed in the outer tube, undergo some initial reactions, vaporize because of the heat released in these reactions, and escape from the tube at sonic velocity. The flame can again be blown off the end of the tube.

### B. Initial Rocket-Motor Tests with Acid-Oxidized Propellant Combinations

In light of the observations described above, it appeared that the concentric-tube configuration could successfully be used as an actual injector element. The 40-lb-thrust scale injector element shown in Fig. 8 was therefore constructed. To enhance the mixing of the propellants, the inner tube was closed at the end and four radial holes, each one-half the tube diameter, were provided. The inner tube was made retractable in order that motor tests could be carried out at different retraction distances. The inner tube could be retracted during any given run. The characteristic exhaust velocities obtained with this injector using SFNA and UDMH were quite high. Tests were carried out at chamber pressures from 150 to 300 psia, and combustion was smooth and stable at all retractions. The chamber had a contraction ratio of about 7:1. Performance first increased with retraction, but then decreased (see Tables 1 and 2). Peak performance as high as 97% of theoretical frozen-flow characteristic exhaust velocity, uncorrected for heat losses to the cooled chamber

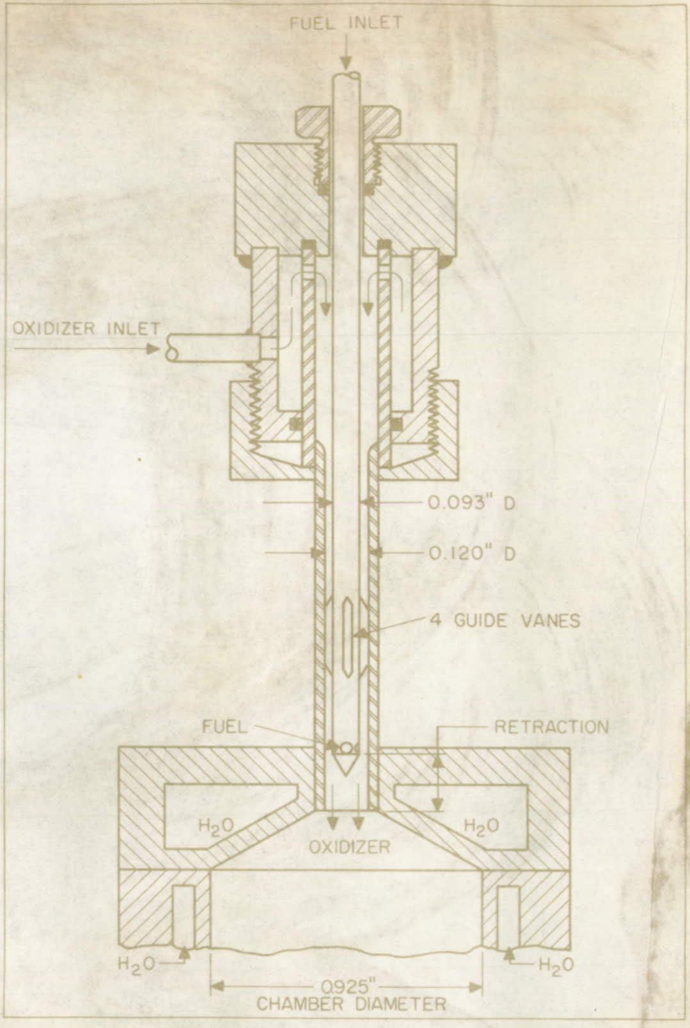


Fig. 8. Four-Hole Concentric-Tube Injector Used with SFNA–UDMH

and nozzle, was obtained at inner-tube retraction of 0.06 to 0.08 in. Optimum mixing at minimum exit velocity apparently takes place at this point. At longer retractions a blowoff condition, such as shown in Plate 18, may occur. Under these conditions the flame probably anchors itself at some point downstream in the chamber where recirculation is strong enough to establish a flame front. During one run, at a retraction of 1.2 diameters, ignition did not occur in the chamber, and no luminous exhaust was observed. The measured characteristic exhaust velocity of 3,759 ft/sec indicated that approximately 50% of the total heat available had been released in the initial reactions. The higher performance levels attained at an $L^*$ of 31 in. (Table 2) are the result of operating at higher mixture ratios and of having a lower heat-transfer correction required compared with the data obtained at 38 in. $L^*$

**Table 1. Performance of 38-in.-$L^*$ SFNA–UDMH Premix Injector**

Contraction ratio = 7
Data uncorrected for heat losses

| Retraction in. | $P_c$ psia | $r$ | $c^*$ ft/sec | $c^*/c^*_{th,fr}$ % |
|---|---|---|---|---|
| 0.02 | 158 | 2.00 | 4870 | 92.7 |
| 0.02 | 182 | 1.91 | 4860 | 92.8 |
| 0.02 | 187 | 1.96 | 4940 | 94.0 |
| 0.02 | 267 | 2.26 | 4965 | 93.7 |
| 0.02 | 301 | 2.08 | 4990 | 94.6 |
| 0.05 | 165 | 2.30 | 4920 | 93.0 |
| 0.06 | 183 | 2.07 | 4935 | 93.8[a] |
| 0.06 | 185 | 2.21 | 5000 | 94.6[a] |
| 0.07 | 288 | 2.04 | 5030 | 95.6 |
| 0.08 | 167 | 1.84 | 4840 | 93.0 |
| 0.08 | 195 | 2.00 | 5030 | 95.8 |
| 0.08 | 269 | 2.23 | 5020 | 95.0 |
| 0.08 | 271 | 2.22 | 5090 | 96.1 |
| 0.09 | 197 | 2.07 | 4925 | 93.6 |
| 0.09 | 235 | 2.00 | 5020 | 95.6 |
| 0.10 | 197 | 2.11 | 4950 | 94.0 |
| 0.10 | 254 | 2.29 | 4940 | 93.2 |
| 0.10 | 257 | 2.09 | 4760 | 90.5[b] |
| 0.10 | 278 | 2.26 | 4945 | 93.4 |

[a]Rough, low-frequency operation.
[b]Very rough, two-level operation.

**Table 2. Performance of 31-in.-$L^*$ SFNA–UDMH Premix Injector**

Contraction ratio = 7
Data uncorrected for heat losses

| Retraction in. | $P_c$ psia | $r$ | $c^*$ ft/sec | $c^*/c^*_{th,fr}$ % |
|---|---|---|---|---|
| 0.02 | 252 | 1.92 | 4730 | 90.7 |
| 0.02 | 255 | 2.26 | 4870 | 92.0 |
| 0.02 | 264 | 1.96 | 4910 | 94.0 |
| 0.02 | 264 | 2.30 | 5020 | 94.7 |
| 0.02 | 270 | 2.47 | 4975 | 93.8 |
| 0.06 | 271 | 2.50 | 5080 | 95.7 |
| 0.06 | 276 | 2.53 | 5150 | 97.1 |
| 0.06 | 278 | 2.57 | 5140 | 96.8 |
| 0.08 | 262 | 2.56 | 5065 | 95.7 |
| 0.08 | 267 | 2.58 | 5130 | 96.8 |
| 0.08 | 269 | 2.64 | 5120 | 96.8 |
| 0.10 | 248 | 2.66 | 4955 | 94.0 |
| 0.124 | 262 | 2.70 | 5010 | 95.0 |
| 0.134 | 266 | 2.53 | 4980 | 94.0 |
| 0.134 | 266 | 2.58 | 4940 | 93.2 |
| 0.159 | 202 | 2.58 | 3750 | 70.7[a] |
| 0.172 | 244 | 2.61 | 4905 | 92.7 |

[a]No luminous flame reaction.

From these results it must be concluded that the oxidation of UDMH by nitric acid consists of two series of reactions, each releasing large quantities of heat. The initial reactions, which vaporize and superheat the propellants, result in intermediate reaction products which are stable enough that they do not undergo further reaction upon being cooled by the expansion from the relatively high pressure in the mixing region to the lower pressure in the combustion chamber. The second series of reactions, which usually result in a luminous flame, cannot proceed under these conditions. If, however, a flame is once anchored in the chamber, it cannot be blown out. Establishment of the luminous flame can be accomplished by starting the motor at a small retraction and then retracting the inner tube under combustion conditions. In this manner retractions in excess of 1.2 diameters can be obtained without the loss of the luminous flame.

### C. Initial Tests with $N_2O_4$–$N_2H_4$ at 40-lb Thrust

In light of the success obtained with the premixing concentric-tube injector using SFNA–UDMH, it appeared that an injector of this type would also yield high performance with $N_2O_4$–$N_2H_4$, which is much more reactive than the former system. The performance of $N_2O_4$–$N_2H_4$ with the four-hole inner-tube injector at zero retraction under conditions similar to those of Section III, however, was low and the combustion was quite rough. This behavior was attributed to the nonuniform mixing and propellant distribution produced by the four-hole injector without premixing. Gross imbalances in the mixture-ratio distribution may give rise to detonable hydrazine-rich mixtures in the chamber and may lead to incomplete combustion. Attempts to retract the inner tube produced sharp explosions occurring at random throughout a test, and finally resulted in destruction of the tubes.

In order to improve the mixing at minimum retraction, the inner tube was modified by the inclusion of a flat distributor at the end of this tube. This configuration at the small scale produced a striated radial sheet of one propellant which apparently penetrated the annular stream of the other propellant. Thus, a fairly uniform mixture-ratio distribution was established, even though some separation of fuel and oxidizer occurred. Some tests were carried out with the fuel in the inner tube and others with the fuel in the annulus. With the inner tube thus modified, a characteristic exhaust velocity of 5,000 ft/sec, which corresponds to 88% of theoretical frozen flow, was obtained at zero retraction with the oxidizer on the inside. Performance could be materially improved by retraction of the inner tube. At a retraction of 1 diameter the characteristic exhaust velocity increased to 5,600 ft/sec, corresponding to 98% of theoretical frozen flow, uncorrected for heat losses.

At almost all retraction distances, however, random explosions occurred in the mixing region which finally resulted in the destruction of the injector. In the process of trying to determine the regions of stable operation of such an injector with premixing, it was discovered that beveling the end of the outer tube at an included angle of 60 deg resulted in both stable operation and high performance even at zero retraction. The final design which has been found to give the best operation is shown in Figs. 9 and 10.

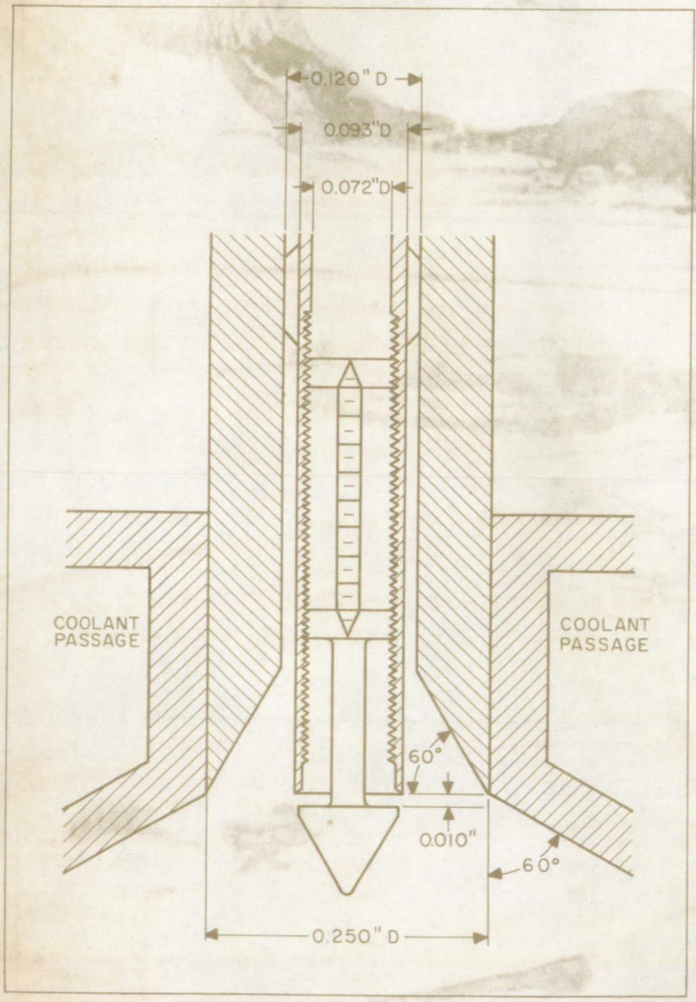


**Fig. 9. Tube Configuration of 40-lb-Thrust Injector Used with $N_2O_4$–$N_2H_4$**

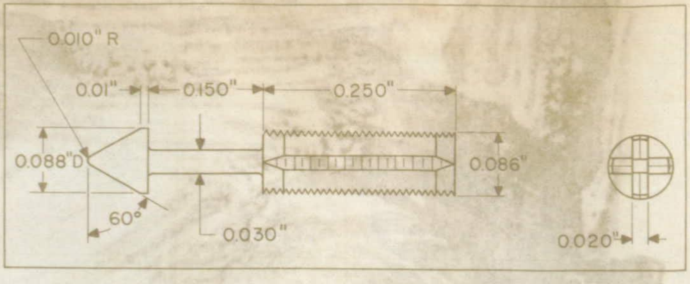


**Fig. 10. Distributor Pin Used in 40-lb-Thrust Concentric-Tube Injector**

The deflector pin (Fig. 10) is fixed in place by screwing it into the threaded inner tube and then crimping the inner tube in a collet. This method of fixing the deflector has been found superior at small scale to all other methods tried, which include soft soldering, silver soldering, gold soldering, and nickel-base brazing the threads inside the tube. The water spray produced with this deflector is much more uniform than that produced by the four-hole inner tube; however, four pronounced streaks are still apparent, as well as many finer variations in mass concentration. Some improvement in the uniformity of the spray probably could be achieved by removing the guide vanes farther upstream, but then the neck holding the head of the distributor would be severely weakened. The four guide vanes which fix the inner tube with respect to the outer tube are cut from a flat sheet and are spot welded to the inner tube. They also disturb the flow pattern, but to a smaller degree than the vanes in the inner tube, as they are located farther upstream. The resultant hollow-cone spray produced by water flowing through both the inner tube and the annulus exhibits mass flow imbalances caused by all eight guide vanes.

The performance as a function of mixture ratio of the concentric-tube injector shown in Fig. 8, modified according to designs shown in Figs. 9 and 10 and using $N_2O_4$–$N_2H_4$, is given in Table 3. A correction to measured $c^*$ values was made for heat transfer using the equation

$$c^*_{\text{corr}} = c^*_{\text{meas}} \sqrt{\frac{\Delta H_{\text{th}} + Q_c}{\Delta H_{\text{th}}}}$$

At 40-lb thrust this correction was appreciable, amounting to about 4%; whereas at the higher thrust levels the magnitude of the corrections falls off rapidly, and they were generally not made. The data were obtained with the fuel in the annulus and the oxidizer in the inner tube.

**Table 3. Performance of 40-lb-Thrust $N_2O_4$–$N_2H_4$ Motor with Concentric-Tube Injector Element**

**Contraction ratio = 7.7**
**Data corrected for heat losses**

| $L^*$ in. | $P_c$ psia | r | $c^*$ ft/sec |
|---|---|---|---|
| 46 | 294 | 0.626 | 5540 |
| | 294 | 0.754 | 5640 |
| | 292 | 0.864 | 5690 |
| | 281 | 0.982 | 5730 |
| | 283 | 0.985 | 5680 |
| | 280 | 1.14 | 5680 |
| 38 | 272 | 0.526 | 5260 |
| | 287 | 0.594 | 5440 |
| | 258 | 0.630 | 5500 |
| | 291 | 0.696 | 5530 |
| | 287 | 0.800 | 5620 |
| | 291 | 0.896 | 5660 |
| | 271 | 0.959 | 5660 |
| | 280 | 0.994 | 5660 |
| | 262 | 1.11 | 5660 |
| | 283 | 1.16 | 5660 |
| | 280 | 1.24 | 5650 |
| 31 | 282 | 0.700 | 5440 |
| | 277 | 0.761 | 5520 |
| | 274 | 0.872 | 5570 |
| | 273 | 0.975 | 5590 |
| | 276 | 1.03 | 5600 |
| | 269 | 1.11 | 5600 |
| | 284 | 1.17 | 5600 |
| 17 | 263 | 0.652 | 5110 |
| | 265 | 0.685 | 5250 |
| | 276 | 0.795 | 5350 |
| | 270 | 0.827 | 5460 |
| | 270 | 0.951 | 5450 |
| | 286 | 1.095 | 5440 |
| | 277 | 1.265 | 5370 |

Reversing the propellants had little effect on the performance at this thrust scale. A comparison of the performance of the concentric-tube element with a two-on-two and a triplet element using the same propellant combination is shown in Fig. 11. Data for the two-on-two and triplet elements are presented in Tables 4 and 5 respectively. At equal chamber lengths and diameters the concentric-tube injector performs considerably better than either of the other two injectors. Since the activation energies of the gas-phase reactions are not dependent on the injector characteristics, one possible explanation for the improvement is that the concentric-tube injector produces a more uniform initial mixture-ratio distribution, which is necessary for complete combustion.

The throttling characteristics of the concentric-tube injector described above with the fuel in the annulus and

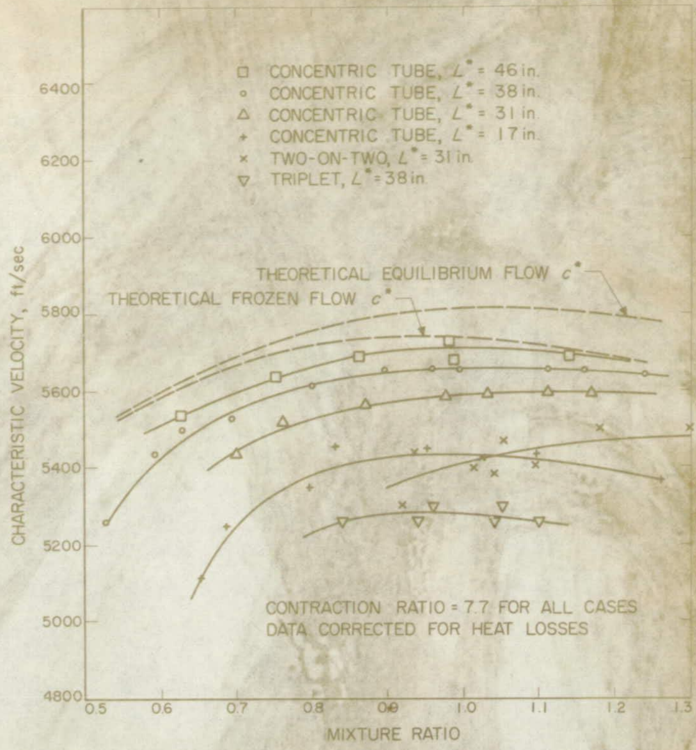


**Fig. 11. Performance Results for $N_2O_4$–$N_2H_4$ Using Several Types of Injector Elements at 40-lb Thrust**

the oxidizer in the inner tube are shown in Fig. 12. In this Figure variations in the chamber pressure were obtained by varying the propellant flow rates at constant nozzle diameter. If the nozzle diameter is changed to a different value, a similar curve with variation in propellant flow rate is obtained. Furthermore, the maximum of this new curve occurs at the chamber pressure corresponding to the same propellant flow rate as the maximum of the

**Table 4. Performance of 40-lb-Thrust $N_2O_4$–$N_2H_4$ Motor with Two-on-Two Injector Element**

**$L^*$ = 31 in.**
**Contraction ratio = 7.7**
**Data corrected for heat losses**

| $P_c$ psia | r | $c^*$ ft/sec |
|---|---|---|
| 228 | 0.918 | 5300 |
| 286 | 0.931 | 5440 |
| 304 | 1.01 | 5400 |
| 289 | 1.04 | 5390 |
| 315 | 1.05 | 5470 |
| 276 | 1.095 | 5410 |
| 297 | 1.18 | 5500 |
| 296 | 1.30 | 5500 |

**Table 5. Performance of 40-lb-Thrust $N_2O_4$–$N_2H_4$ Motor with Triplet-Injector Element**

$L^* = 37$ in.

| $P_c$ psia | $r$ | $c^*$ ft/sec |
|---|---|---|
| 162 | 1.04 | 5300 |
| 214 | 1.10 | 5260 |
| 218 | 1.05 | 5300 |
| 258 | 0.97 | 5300 |
| 277 | 0.95 | 5260 |
| 254 | 0.83 | 5260 |

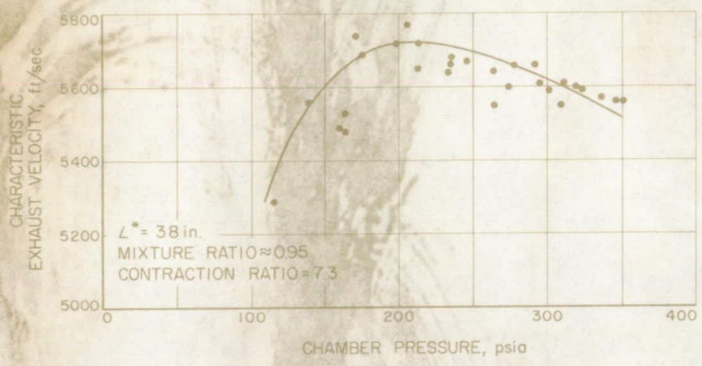


**Fig. 12. Performance of 40-lb-Thrust $N_2O_4$–$N_2H_4$ Concentric-Tube Injector as a Function of Chamber Pressure**

curve in Fig. 12. Hence, it follows that the variation in the characteristic exhaust velocity with chamber pressure is due to changes in the mixing characteristics produced by variations in the injection velocities, rather than due to any pressure dependence of the chemical reactions involved. It appears, therefore, that at least for this injector-propellant combination, optimum injection velocities exist. On the oxidizer side, 25 ft/sec is required, and on the fuel side 30 ft/sec is required. The velocity-head pressure drops corresponding to these velocities are 9 and 4.2 psi, respectively. Pressure drops of this magnitude are easily varied over a large ratio, even in pressure-fed systems.

The combustion was found to be smooth and stable at all pressures and at all chamber lengths. No damage of any sort to the injector was noted, even though the injector had been started well over one hundred times and had been run for a cumulative time of about 45 min. Starting was accomplished without the use of any auxiliary means such as flushing the injector with nitrogen or with water. During shutdown the injector and the propellant lines downstream of the fire valves were flushed with water to prevent the propellants from dripping into the combustion chamber after the conclusion of the run. Whether such a shutdown procedure is really required has not been investigated. It is suggested that the necessity of flushing the injector during shutdown be investigated specifically for each injector configuration.

Heat transfer to the injector face plate was found to be minimal. The over-all heat-transfer rate to the injector was approximately 0.1 Btu/in.$^2$ sec. The heat transfer in the chamber was also low. The value predicted by the method described in Ref. 5 for the combustion chamber is 30% higher than the rate actually measured. This is quite significant, especially in light of the fact that the predictions made by Bartz's method are normally too low for thrust chambers with high contraction ratios. Apparently the regions adjacent to the chamber walls for some distance downstream of the impingement point are rich in hydrazine (the propellant in the annulus in this series of tests). This could give a relatively cool boundary layer which mixes downstream to complete the combustion. In addition, the rapidly expanding vapors from initial reactions quickly fill the cross-sectional area of the chamber so that little recirculation of very hot gases occurs. Thus, the heat transfer to the chamber walls is materially decreased over the initial region of the chamber. Presumably, if the oxidizer is in the annulus, a decreased heat-transfer rate due to a boundary layer rich in $N_2O_4$ will be observed.

## D. Open-Flame Studies of $N_2O_4$–$N_2H_4$

In order to understand the combustion of the $N_2O_4$–$N_2H_4$ propellant combination and to find out why premixing was unattainable with this system, a series of open-flame tests was made. The study of open flames with this system is particularly instructive as the intense dark brown color of nitrogen tetroxide identifies regions of the flame rich in this component. Regions rich in hydrazine are identified by the colorless liquid itself, or a yellow flame which is characteristic of hydrazine-rich combustion.

*1. Knife edge.* The characteristics of the streams produced by a set of knife-edge concentric tubes at zero retraction with $N_2O_4$ in the inner tube and $N_2H_4$ in the annulus are shown in Plate 20. In the picture the brown core consists primarily of the oxidizer and the bright streaks are mainly droplets of hydrazine. The extent of reaction between the two propellants is exceedingly slight, and the luminous flame is almost completely absent. This behavior of the streams is quite unexpected in light of the fact that with less reactive systems, such as the ones shown in Plates 17 to 19, much more reaction takes place under identical injection conditions.

The differences in behavior may be explained in terms of the rates of the initial reactions of the various propellant systems. With relatively slow reacting systems, such as SFNA–JPX and SFNA–UDMH, there is an ignition delay time of the order of a few milliseconds. That is, combustion is not initiated until a few milliseconds after the propellants have come into contact. During this time interval liquid-phase mixing may take place. The mixed liquids then react in the liquid phase until enough heat is generated to vaporize the propellants and to bring the reaction products to their ignition point. The vapors and gases generated in this manner then serve to atomize whatever liquid is still present. The resultant liquid-vapor mixture then undergoes combustion.

With $N_2O_4$–$N_2H_4$ the reaction delay appears to be exceedingly short. No measurement of its exact value has been made; however, from various tests it can be estimated that the delay time is much less than 1 millisec. During such a short time interval very little liquid-phase mixing can take place. As the two propellants come in contact, some reaction takes place almost immediately, and the gaseous reaction products may form an expanding inert buffer between the propellants. Thus, additional interaction between the propellants could be prevented and the fuel and oxidizer streams would diverge without undergoing further combustion. The differences in the combustion characteristics of the systems considered may thus be due to differences in the delay times of the initial energetic reactions.

Under some conditions the inner tube may be retracted into the outer one to provide a confined mixing section. Under these conditions the high-velocity liquid-vapor mixture escaping from the mixing section consists of a hard core of oxidizer surrounded by a mantle of fuel. In this case the propellants may react upon contact within the outer tube, and the gases generated in the initial reactions could cause lamination of the fuel and the oxidizer, thus preventing further reaction. The gas layer separating the two propellants seems to be very unstable. Under most conditions of premixing, the gas layer breaks down and allows further contact and reaction, which again results in the formation of gases at the interface, accompanied by some heat release. With each successive burst of reaction, the temperature of the propellants and the pressure within the mixing zone are increased. Eventually the temperature and pressure reach high enough values to cause explosive decomposition of the hydrazine and any intermediate reaction products that may be present. From the damage inflicted upon the mixing tube it can be estimated that peak pressures as high as 50,000 psi are generated within the mixing zone. Because of pressure surges of such magnitude, the propellant flows are completely stagnated, which results in an increase in the time of residence of the still uncombusted propellants in the mixing zone. With sufficient time for reaction, a zone of high pressure and temperature is again established, giving rise to explosive decomposition. Thus, one disturbance can trigger a whole series of explosions. The behavior with the propellants reversed is identical. From the above observations it is apparent that premixing of $N_2O_4$ and $N_2H_4$ with a set of knife-edge concentric tubes is not feasible. Either the reaction proceeds with destructive violence or, if steady operation is somehow established, the propellants escaping from the mixing section are laminated to such a degree that complete combustion is not possible in any reasonable chamber length.

*2. Deflector.* The extent of mixing between the propellants can be greatly enhanced by providing a deflector at the end of the inner tube, such as the one shown in Figs. 9 and 10. The deflector effectively redirects the component in the center tube so that it impinges at right angles on the component in the annulus. A maximum degree of penetration of the two propellant films is expected with such a geometry. The characteristics of the flame produced by a set of concentric tubes with such a deflector at the end of the inner tube are shown in Plate 21. In this photograph the oxidizer is in the annulus and the fuel is in the center tube. Compared to the streams produced without the deflector (Plate 20) there is a marked increase in the extent of reaction. A fair amount of separation is, however, still evident. The fuel is forced predominantly to the inside while some of the oxidizer forms a mantle around the flame. Apparently, a large enough quantity of heat is released during the initial reactions to vaporize most of the oxidizer. However, since the fuel has a considerably higher heat of vaporization, it is not completely vaporized, and streaks characteristic of burning fuel droplets are apparent in the photograph. Some of these burning droplets appear to penetrate through the mantle of vaporized oxidizer. The average local mixture ratio within the mantle is therefore not as high as it appears at first glance.

The characteristics of the flame are not materially affected by the presence of a flat injector face plate, as shown in Plate 22. The degree of separation of the two propellants appears to be unchanged. The large droplet hanging from the bottom of the injector face plate is hydrazine that has been sprayed through the oxidizer mantle and has accumulated on the injector face plate. The temperature of this hydrazine is apparently not high enough to cause spontaneous decomposition; instead, the hydrazine burns in air and nitrogen tetroxide vapor with a diffusion flame.

From Plate 22 it appears that a more uniform mixture-ratio distribution may be established by redirecting the excess oxidizer surrounding the flame in such a manner that it has to pass through the flame where it can react with excess fuel. This may be conveniently accomplished by the addition of a short chamber section to the injector face plate. Plate 23 shows the operation of the injector described above with a 0.15-in.-long, 0.925-in.-diameter chamber section. The mixture-ratio distribution in this flame shows great improvement over that without the chamber section. However, some oxidizer concentration on the outside of the flame and some streaks due to burning hydrazine droplets are still present. As in the two previous photographs, the center portion of the flame is marked by the surrounding luminous reaction zones. The liquid streams at the bottom of the chamber are due to water used for cooling the combustion chamber section.

The true character of this flame can be seen more clearly in Plate 24, which shows the operation of the injector with a 1.0-in.-long, 0.925-in.-diameter chamber. The fuel is again in the center tube and the oxidizer is in the annulus. Because of the absence of a large luminous combustion mantle, the center portion of the flame can be seen quite clearly. A possible interpretation of the picture is that the flame consists essentially of three parts: a relatively cool hydrazine-rich core located in the center; oxidizer present in relatively high concentrations in the outer portions of the flame; and a zone of highly luminous reaction in between. Streaks due to burning hydrazine droplets are no longer present. Apparently, a large enough quantity of heat is generated by the reactions of the mixed liquids within the chamber section to bring about nearly complete vaporization. Combustion then proceeds toward completion by vapor-phase reactions.

By sufficiently increasing the propellant flow rates, the pressure within the 1-in.-long chamber section can be raised high enough so that sonic flow is reached at the open end of the chamber. Under such conditions the approximate value of the characteristic exhaust velocity may be determined by measuring the propellant flow rates and the chamber pressure at the injector end. An appropriate correction for the velocity head can then be made with reasonable accuracy. In this manner, characteristic exhaust velocities of about 4,800 ft/sec were obtained with fair reproducibility. This means that with a characteristic length $L^*$ of only 1 in., approximately 70% of the total available heat release has taken place. The gas-phase residence time, which is related to the characteristic chamber length, therefore can not be an important parameter in determining over-all performance. The rate of initial mixing and the uniformity of the mixture-ratio distribution within the combustion chamber appear to be of much greater importance in determining the performance level in motors having an $L^*$ of more than a few inches.

The next series of three photographs, Plates 25 through 27, were taken under the same conditions as Plates 22 through 24, except that the positions of the fuel and oxidizer were reversed. In Plates 25 through 27 the fuel is in the annulus and the oxidizer in the inner tube.

In Plate 25 the quantity of fuel accumulated on the injector face plate appears to be far in excess of the amount of oxidizer present in the same region in Plate 22. This is probably a result of the fact that hydrazine has a boiling point and heat of vaporization high enough that accumulation of the liquid may take place, while the oxidizer is entirely vaporized. The degree of separation of the propellants upon contact is therefore probably about equivalent in the two cases.

It is interesting to note that the hydrazine accumulated on the injector face plate in Plate 25 is quite stable and does not decompose explosively, even though it is in contact with vaporized oxidizer and is boiling vigorously. It appears from this observation that in an unconfined region hydrazine is not prone to decompose explosively.

Plates 26 and 27 show the same general flame characteristics and the same degree of maldistribution in mixture ratio as the corresponding flames with the propellants reversed. From this it follows that the performance with the fuel and oxidizer in different positions should not be expected to be markedly different, at least at this scale. This has actually been observed experimentally.

These results of the behavior of the $N_2O_4$–$N_2H_4$ propellant system in concentric-tube elements support the hypothesis previously advanced for impinging streams; namely, that the initial reactions between these propellants are so fast that good liquid-phase mixing is prevented by a layer of expanding gaseous reaction products formed at the liquid-liquid interface immediately upon contact.

In addition, the open-flame tests with $N_2O_4$ and $N_2H_4$ suggest several other principles governing their combustion:

1. The initial reactions between the $N_2O_4$ and $N_2H_4$ which do mix release sufficient heat to vaporize a substantial portion of the propellant mixture.
2. Forced liquid-phase mixing in a very confined volume is not feasible because of the formation of detonable fuel-rich mixtures.
3. The important parameters in determining the completeness of combustion are the rate of initial mixing and the uniformity in mixture-ratio distribution. The characteristic chamber length appears to be relatively unimportant over the range tested.

The results of the open-flame tests described above left some hope that forced turbulent secondary mixing in a relatively unconfined volume may be exploited as an injection technique. If just enough volume is provided for the escape of the gases generated during the initial reactions, a stable mixing region might be maintained in which the propellants can be further mixed prior to injection into the main motor chamber. Combustion can then be carried to completion by vapor-phase reactions in the combustion chamber proper. Accordingly, an injector using the exact tube configuration shown in Figs. 9 and 10 was constructed with a 0.75-in.-long mixing section equal in diameter to the nozzle throat (0.333 in). Tests were carried out with the inner tube retracted to different positions within this mixing section. The characteristic exhaust velocity as a function of retraction distance is shown in Fig. 13. For comparison, the performance at the same characteristic chamber length $L^*$ and at the same total chamber length, including the mixing section, are also included. The relatively low performance at zero retraction is a result of the fact that the fuel, the com-

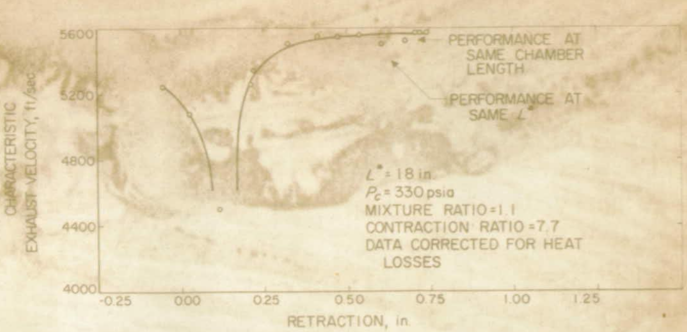


**Fig. 13. Performance of 40-lb-Thrust $N_2O_4$–$N_2H_4$ Motor with Concentric-Tube Injector Element as a Function of Retraction into a Mixing Section**

ponent in the annulus, has to traverse the entire length of the mixing section as a free stream. Any initial annular unsymmetrical distribution is magnified in the free stream, and a nonuniform mixture-ratio distribution can result. The sharp decrease in the characteristic exhaust velocity with initial retraction is probably caused by partial impingement and condensation of the deflected hydrazine on the mixing section walls, resulting in less oxidizer penetration. With additional retraction, turbulent mixing and vaporization overcome the initial separation.

It can be seen from Fig. 13 that a slight improvement in the performance is realized over that obtainable in the same total chamber length without the mixing section. The pressure drop in the mixing section at full retraction is, however, about 150 psi, which makes this method of improving the performance impractical. In light of this fact, premixing in a relatively unconfined mixing section was abandoned as an injection technique.

### *E. Motor Tests with $N_2O_4$–$N_2H_4$ at 80-lb Thrust*

Based on the successful operation of the 40-lb-thrust injector, an 80-lb-thrust element was designed, built, and tested. The scale-up was made by increasing all pertinent linear dimensions of the 40-lb-thrust element by a factor of $\sqrt{2}$. Thus, all flow areas were increased by a factor of 2 and the injection velocities were unchanged. The limited data obtained with this element with hydrazine in the center tube are plotted in Fig. 14. It is worthwhile noting that characteristic exhaust velocities close to theoretical frozen flow were obtained even though the characteristic chamber length $L^*$ was only 12 in. Here again is further evidence that the characteristic chamber length is not the parameter governing the completeness of the combustion in a rocket motor.

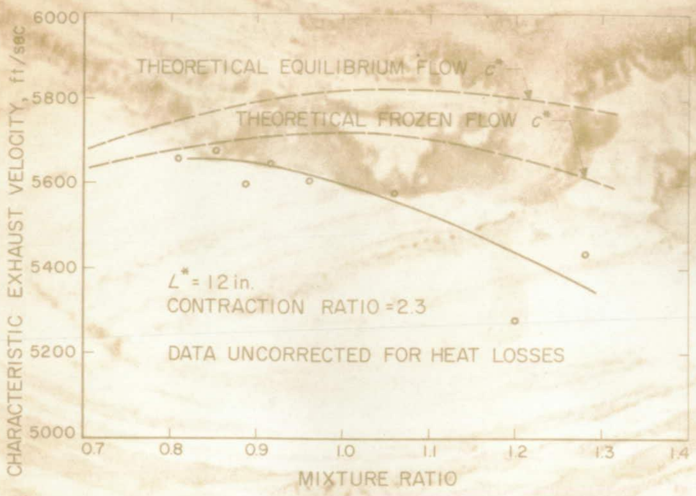


**Fig. 14. Performance of 80-lb-Thrust $N_2O_4$–$N_2H_4$ Motor with Concentric-Tube Injector Element**

## F. Motors Tests with $N_2O_4$–$N_2H_4$ at 800-lb Thrust

In order to determine the effect of large variations in element size, an element was geometrically scaled from 40-lb to 800-lb thrust. The resultant 800-lb element is shown in Figs. 15 and 16. The two major deviations from an exact geometrical scaling lie in the design of the propellant feed passages and in the different method of fixing the deflector pin at the end of the inner tube. The feed passages were redesigned to allow the establishment of stabilized turbulent velocity profiles in the annulus in a comparatively short distance. The method of fixing the deflector pin used at the 40-lb-thrust scale—namely, threading and crimping the inner tube—was found to be insufficient to withstand the high level of vibration encountered in the first few tests with the 800-lb injector. The pin was therefore fixed by means of a long rod located in the center of the inner tube. This rod was brought out of the inner tube through an elbow and was silver soldered there. It was spaced with respect to the inner tube by means of three guide vanes. It was found that no appreciable disturbance in the flow pattern results if the vanes are located at least 1 in. upstream of the deflector pin.

The geometrically scaled element with the tube design of Fig. 15 produced unexpectedly rough combustion and performance that was only a little better than that obtained with a two-on-two element at this thrust level. The following presents a possible explanation for these results:

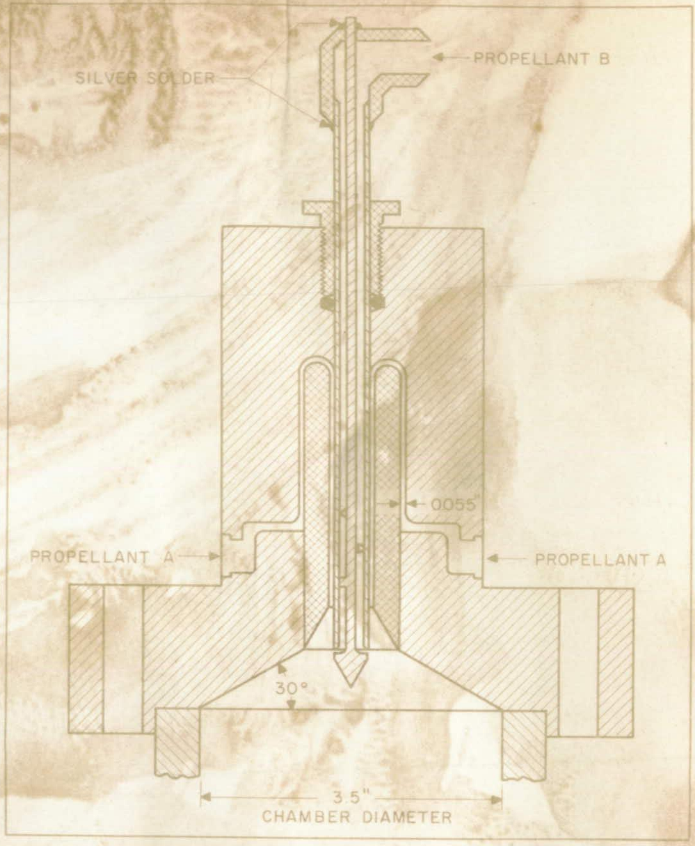


**Fig. 15. 800-lb-Thrust Concentric-Tube Injector with Original Tube Configuration**

At the larger scale the element produces thicker and more nearly uniform propellant sheets. As these sheets are allowed to impinge on each other, only a very small amount of liquid-phase mixing can take place before large enough quantities of gas are generated to cause lamination of the two propellants. At the 40-lb scale, where the propellant sheets are comparatively thin and streaked, a larger fraction of the total propellants available can take part in the initial mixing and reaction. At the 800-lb scale, however, owing to the uniformity in thickness and in momentum profile of the propellant sheets, no preferred points for the escape of the gases generated in the initial reactions exist. The propellants are therefore more or less uniformly forced apart, which results in a greater percentage of the total propellant being unmixed. Any further mixing between the propellants has to take place downstream in the combustion chamber by diffusion and recirculation, which is a relatively slow process. The lower performance at the larger scale can thus be traced to the thicker and more uniform propellant sheets.

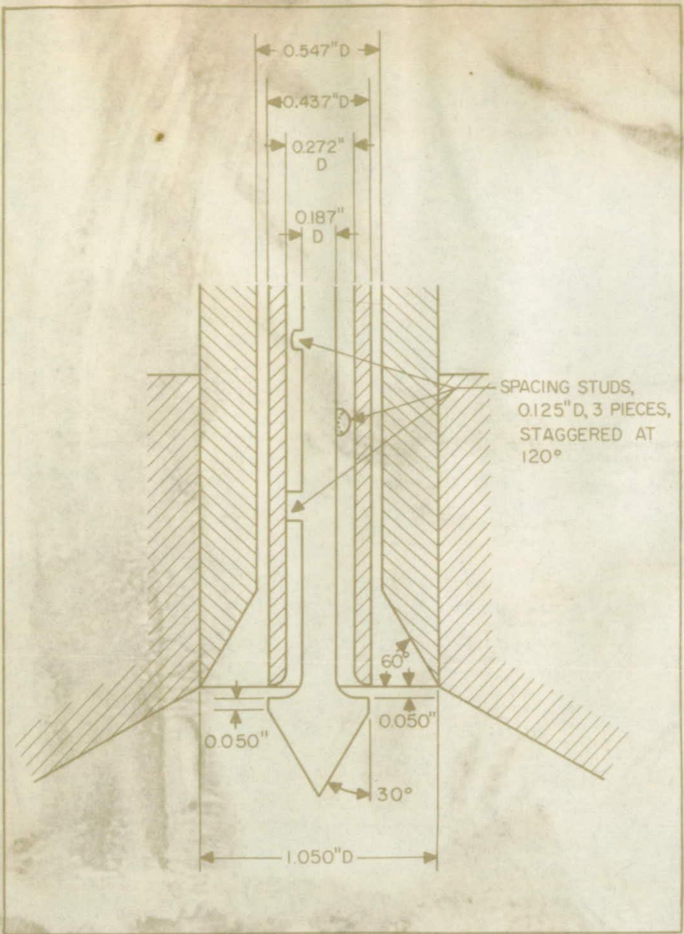


**Fig. 16. Original Tube Configuration of 800-lb-Thrust Concentric-Tube Injector**

The rough combustion, also, may be a direct product of the lamination of the propellants since comparatively large pockets consisting mainly of one component or the other appear to be formed. Pockets consisting predominantly of nitrogen tetroxide only serve to lower the over-all performance, but do not contribute to rough combustion. When fuel is on the outside, it is believed that pockets consisting mainly of hydrazine vapor and partially oxidized hydrazine, confined between the oxidizer flow and the chamber walls, undergo explosive decomposition and thus give rise to large local pressure fluctuations. In the impingement zone the pressure fluctuations are so large and so violent that they severely disturb the propellant flows and prevent the establishment of steady-state conditions. In fact, under some conditions the violence of these explosions is so great that the propellant flows are completely stagnated. An oscillograph record of a motor test showing the primary fluctuations in the chamber pressure and the induced fluctuations in the injection pressures is shown in Fig. 17.

Two methods of coping with the problem of rough combustion and low performance appeared to be feasible. First, the impingement zone can be removed from the points of injection of the propellants so that fluctuations of the local pressure within the impingement zone cannot disturb the propellant flows. Second, some controlled and reproducible nonuniformity in the thickness of at least one of the propellant sheets can be introduced in order to allow penetration of one propellant into the other.

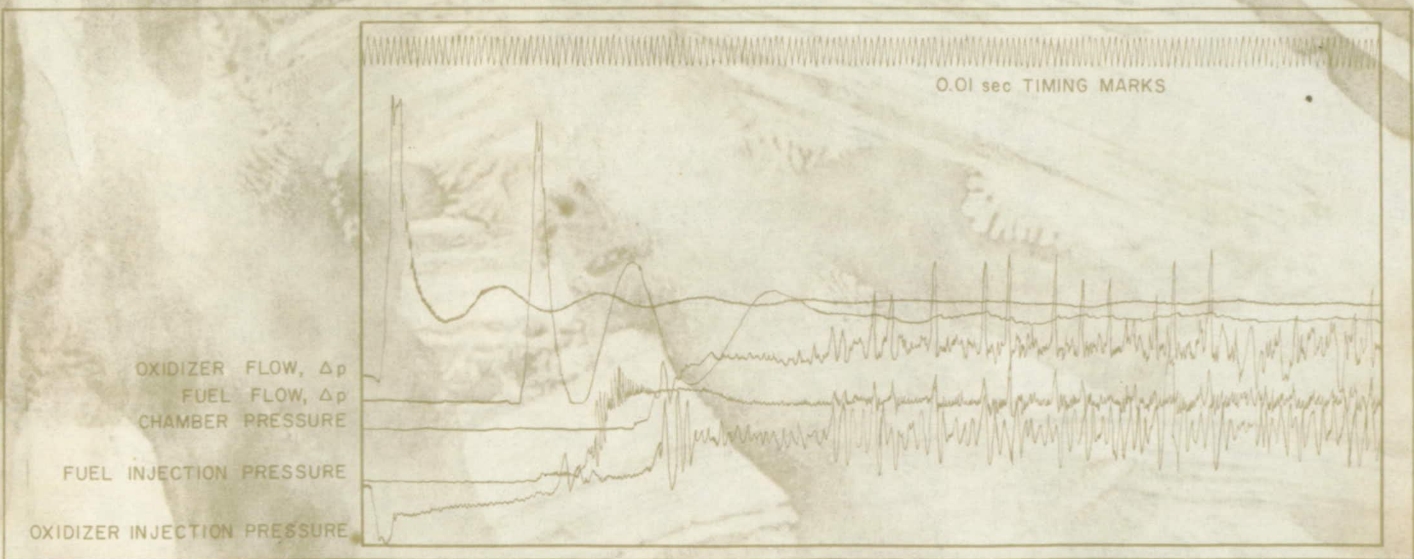


**Fig. 17. Oscillograph Record of 800-lb-Thrust $N_2O_4$–$N_2H_4$ Motor Test with Injector Shown in Fig. 16**

In order to meet the first requirement, the tube configuration of the 800-lb-thrust injector in Fig. 15 was modified according to Fig. 18. The propellant in the annulus now forms a hollow cone which intercepts the radial sheet of the other propellant approximately ½ in. away from the injector face plate. Both of the propellant passages are shaped in such a manner that the cross-sectional flow area decreases with distance measured in the direction of flow just prior to injection. This insures more stable streams and full flow under all conditions. The flow areas can easily be varied by changing the position of the deflector pin with respect to the inner tube.

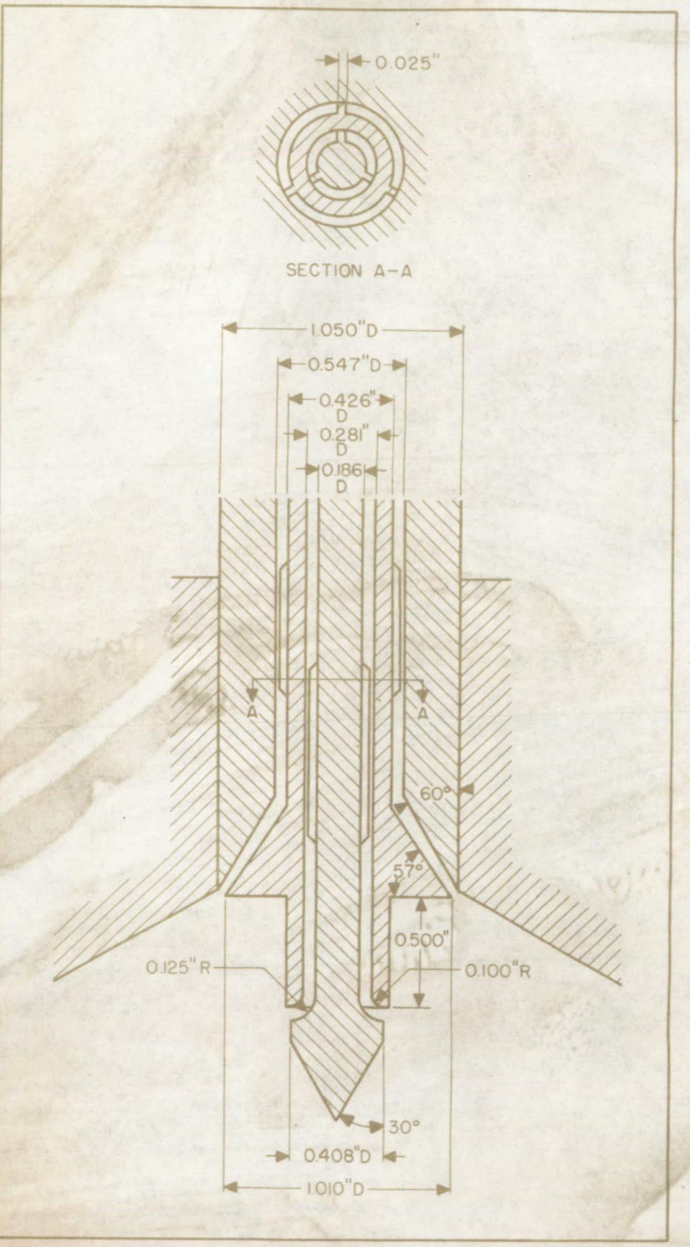


**Fig. 18. Modification No. 1 of Tube Configuration of 800-lb-Thrust Concentric-Tube Injector**

In a series of experiments it was found that this injector operates stably only with the fuel in the inner tube, and then only if the oxidizer injection velocity is less than approximately 40 ft/sec. If the fuel is in the annulus, a large accumulation of hydrazine on the injector face plate and on the chamber walls takes place. The heat generated in the combustion chamber quickly brings this hydrazine to a high enough temperature that it decomposes explosively, giving rise to severe chamber pressure fluctuations. Apparently, the same type of phenomenon occurs if the oxidizer injection velocity is too high. In this case a great deal of fuel is forced to the center of the chamber and there undergoes explosive decomposition.

The performance of this injector at various propellant sheet thicknesses is shown in Fig. 19. Only data corresponding to stable operation are reported. The combustion with this injector is extremely smooth when operating with the fuel in the inner tube and with low oxidizer-injection velocities. An oscillograph record showing the operation of the injector is reproduced in Fig. 20. It seems that removal of the impingement cone from the points of injection of the propellants does actually result in greater stability; however, the absolute performance is still relatively low. Apparently a great deal of separation is taking place upon initial contact of the propellant sheets. It is interesting to note that all performance data points fall on a single straight line, even though they correspond to widely different injection conditions. No correlation is obtained if the data are replotted vs velocity ratio, momentum ratio, or either of the injection velocities. From this it follows that the shape of the curve in Fig. 19 is determined purely by the mixture ratio and is not dependent upon the injection velocities or momentum.

In an attempt to obtain high performance as well as smooth combustion, the 800-lb-thrust element was modified to meet both requirements outlined above. This modification is shown in Fig. 21. The impingement zone is removed from the points of injection by pushing the inner tube some distance out into the chamber. It was found that extending the inner tube beyond ⅛ in. had little effect on the performance and the combustion stability. In order to achieve better penetration of fuel into oxidizer, 24 triangular saw teeth with a 30-deg included angle were cut in the end of the inner tube and the

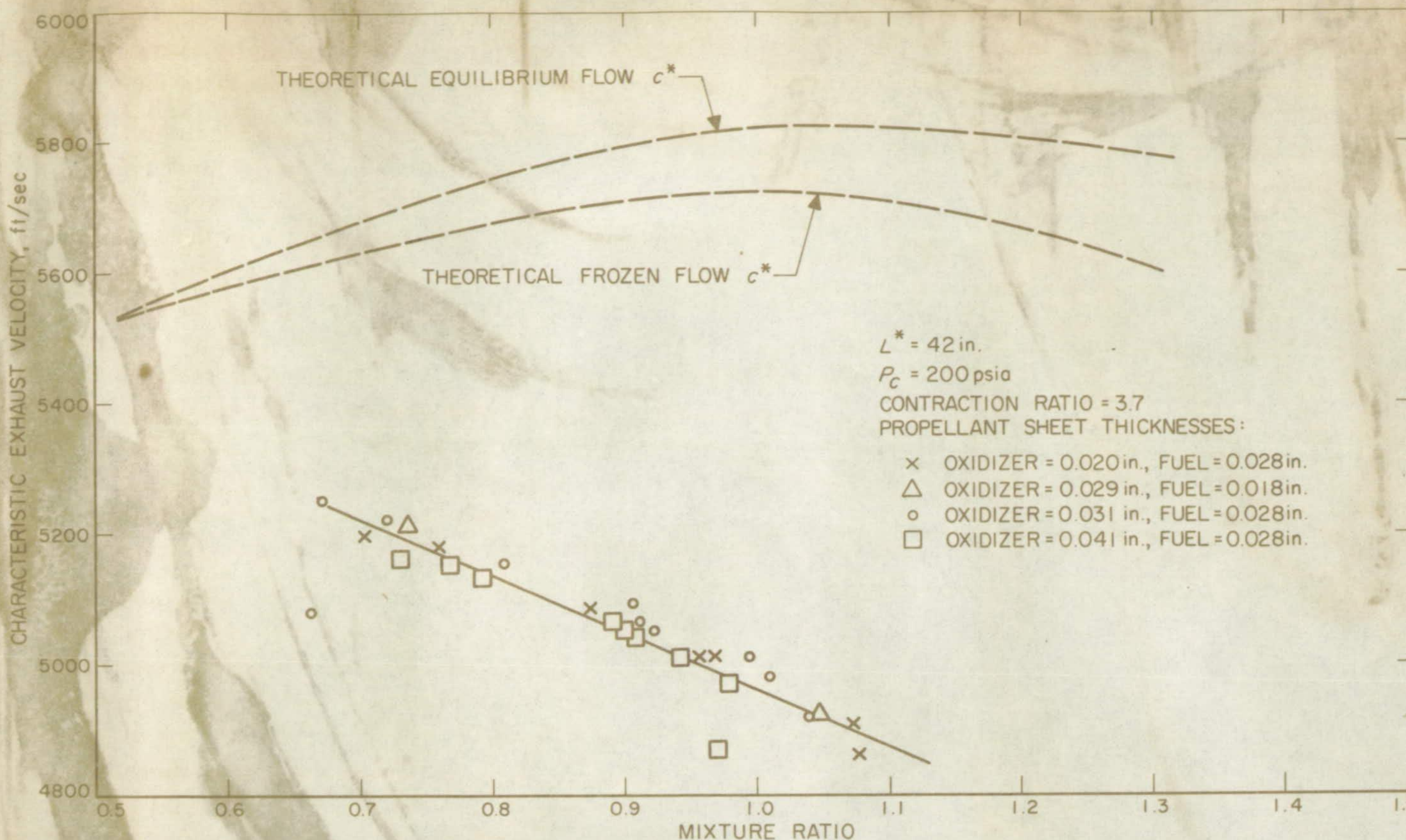


**Fig. 19. Performance of 800-lb-Thrust $N_2O_4$–$N_2H_4$ Motor with Concentric-Tube Injector Element Shown in Fig. 18**

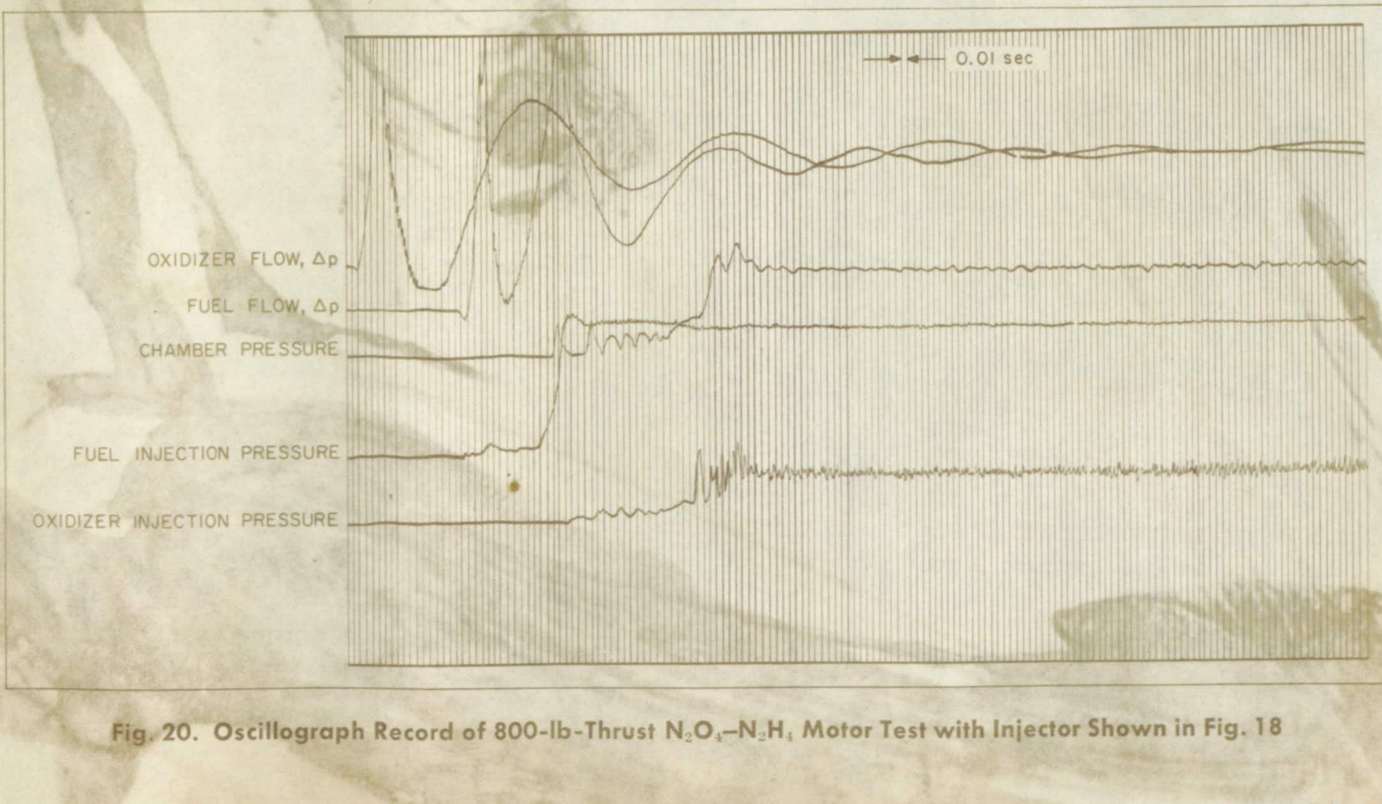


**Fig. 20. Oscillograph Record of 800-lb-Thrust $N_2O_4$–$N_2H_4$ Motor Test with Injector Shown in Fig. 18**

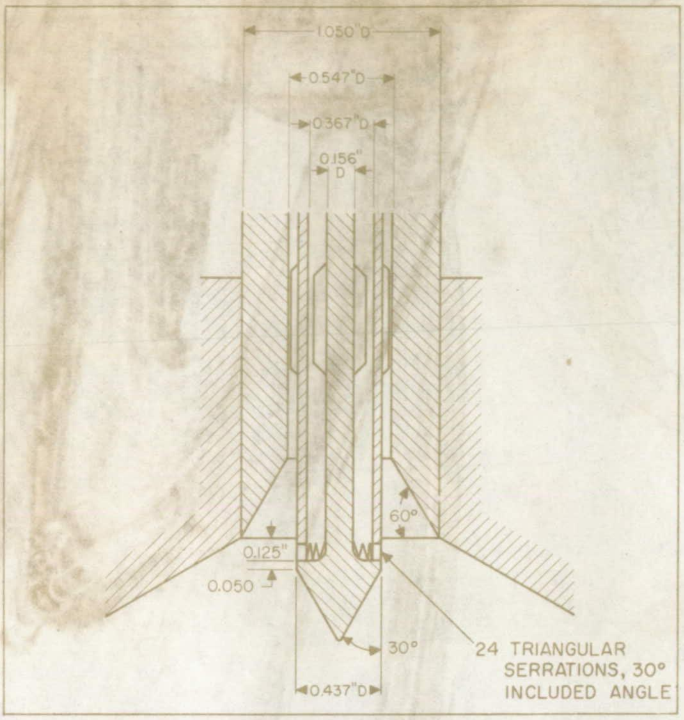


**Fig. 21. Modification No. 2 of Tube Configuration of 800-lb-Thrust Concentric-Tube Injector**

deflector pin was fixed at the end of these teeth. In this manner the continuous annular sheet of oxidizer is intercepted by 24 relatively distinct streams of fuel. A great deal of penetration is thus obtained. Some of the gases produced upon initial contact can escape between the streams without materially laminating the propellants. In fact, the oxidizer and fuel may both be atomized and distributed fairly evenly in all directions by these expanding vapors.

The performance of this injector with the inner tube extended ⅛ in. into the chamber is shown in Fig. 22. An oscillograph record showing the stability of the combustion is reproduced in Fig. 23. The chamber-pressure fluctuations with this modification are somewhat larger than those with the injector of Fig. 18; however, the fluctuations are well within tolerable limits for a single element, about ±5–8% of steady state pressure. The performance of this injector as measured by the percentage of theoretical characteristic velocity is extremely high, especially at low mixture ratios. It can be seen that if the test data were corrected for heat losses, several of the experimental points would lie above the frozen flow curve.

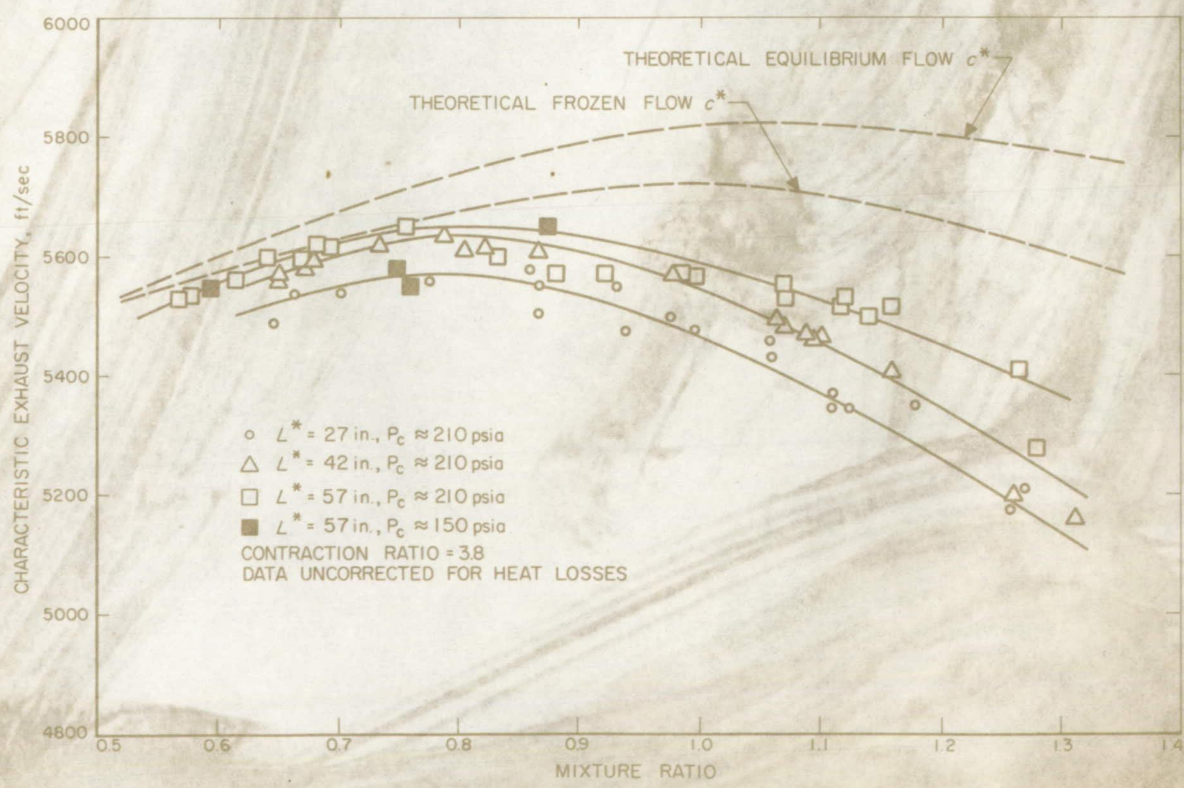


**Fig. 22. Performance of 800-lb-Thrust $N_2O_4$–$N_2H_4$ Motor with Concentric-Tube Injector Element Shown in Fig. 21**


**Fig. 23. Oscillograph Record of 800-lb-Thrust $N_2O_4$–$N_2H_4$ Motor Test with Injector Shown in Fig. 21**

In order to optimize the performance of this type of injector, the number of saw teeth at the end of the inner tube was varied. With 16 teeth the injector operated very roughly and at low performance under all conditions. Possibly, the 16 streams penetrate completely through the oxidizer, and an accumulation of hydrazine at the chamber walls occurs. This hydrazine may then decompose explosively, giving rise to rough combustion. A modification with 32 saw teeth was also tested. Here the combustion was smooth, but the characteristic exhaust velocities were 150 to 200 ft/sec lower than those obtained with the 24-tooth inner tube. In addition, the pressure drop across the teeth was excessive. It is suggested that further work be carried out to optimize this type of injector, with emphasis on improving the performance at high mixture ratios.

# VII. CONCLUSIONS

The experimental results summarized in this report show that for certain propellants the rate of vaporization and therefore the combustion profile in rocket motors can be controlled by the reactions occurring in the liquid phase. For most acid-oxidized systems some slight delay occurs between mixing and rapid self-vaporization. Thus, uniform mixture-ratio distributions can be obtained by various methods such as impinging streams and premixing.

The successful operation of the very reactive systems $N_2O_4$–$N_2H_4$ and $ClF_3$–$N_2H_4$, however, appears to require special techniques for obtaining uniform penetration of the hydrazine into the oxidizer. This mixing must be done rapidly and completely if hydrazine vapor explosions are to be prevented. These hypotheses are supported both by photographic studies of open flames and by performance data obtained in recent motor tests over a thrust range from 40 to 800 lb per element. With impinging streams, this effect can be accomplished through the use of a splash plate or by means of some other method of forced secondary mixing. An alternative technique is to force penetration of fuel into an annular sheet of oxidizer, as in the various concentric-tube designs experimentally investigated in this study.

By using injector elements for reactive propellants which produce on a macroscale a uniform initial mixture-ratio distribution and maximum liquid-phase mixing, high performance can be expected with a minimum number of such elements at any total thrust level.

# NOMENCLATURE

$c^*$ = characteristic exhaust velocity, ft/sec.

$c^*_{th,\,eq}$ = theoretical characteristic exhaust velocity based on equilibrium flow.

$c^*_{th,\,fr}$ = theoretical characteristic exhaust velocity based on frozen flow.

$\Delta H_{th}$ = enthalpy of reaction from thermodynamical calculations.

$L^*$ = characteristic chamber length, in.

$p$ = pressure fluctuation.

$P_c$ = chamber pressure, psia.

$Q_c$ = heat transfer from injector face to throat.

$r$ = mixture ratio (oxidizer/fuel).

Plate 1. Triplet Injector Element Using SFNA–JPX at Non-optimum Stream-Velocity Ratio (Oxidizer Rich)

Plate 2. Triplet Injector Element Using SFNA–JPX at Near-optimum Stream-Velocity Ratio

Plate 3. Two-on-Two Injector Element Using SFNA–JPX at Near-optimum Stream-Velocity Ratio

Plate 4. Two-on-Two Injector Element Using SFNA–UDMH at Near-optimum Stream-Velocity Ratio

Plate 5. Two-on-Two Injector Element Using $N_2O_4$–UDMH at Fuel-Rich Mixture Ratio for Non-optimum Mixing

Plate 6. Two-on-Two Injector Element Using $N_2O_4$–UDMH at Oxidizer-Rich Mixture Ratio for Non-optimum Mixing

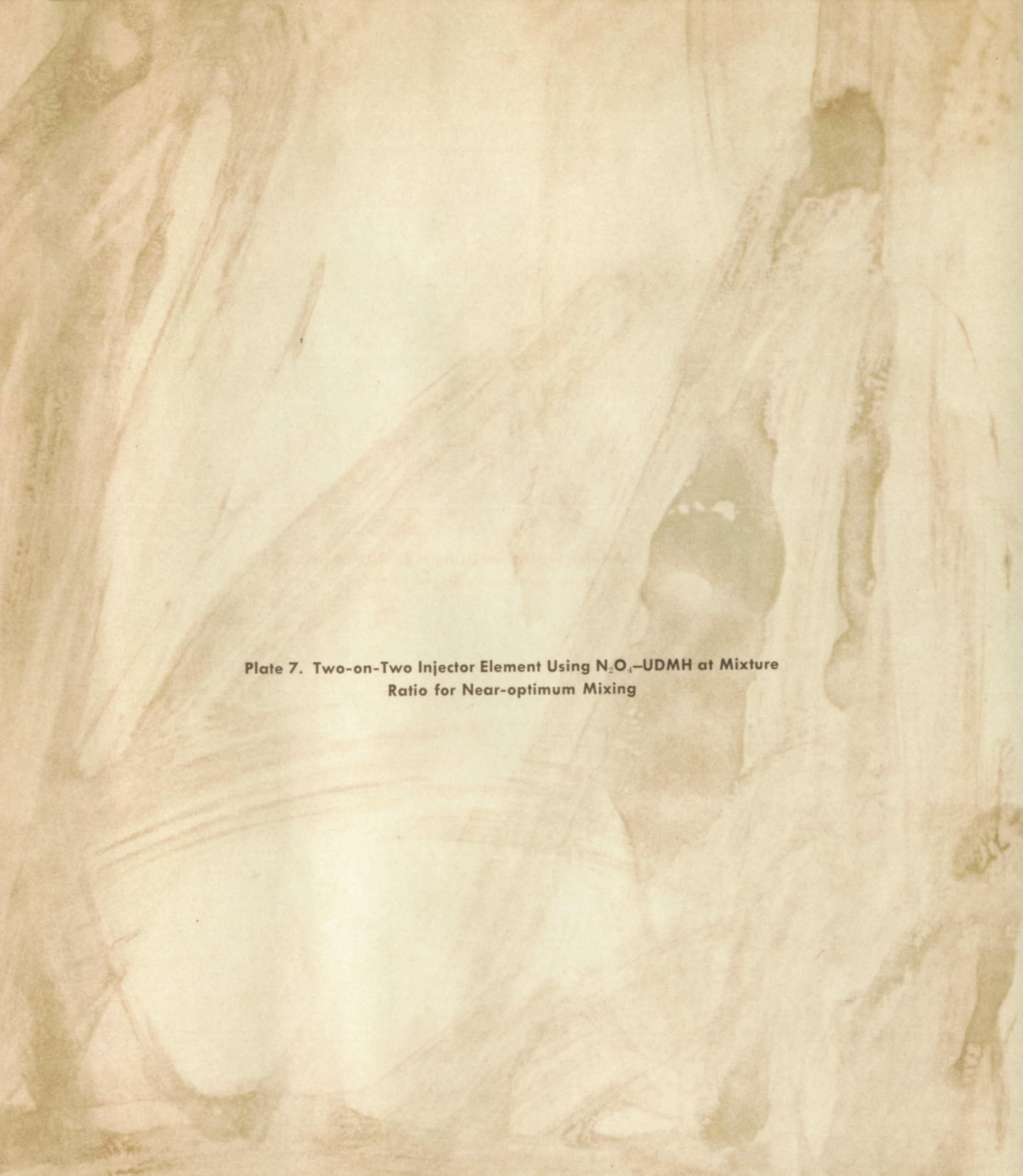

Plate 7. Two-on-Two Injector Element Using $N_2O_4$–UDMH at Mixture Ratio for Near-optimum Mixing

Plate 8. Concentric Water Streams Impinging on Flat End of Rod, Showing Inert-Liquid Spray Pattern

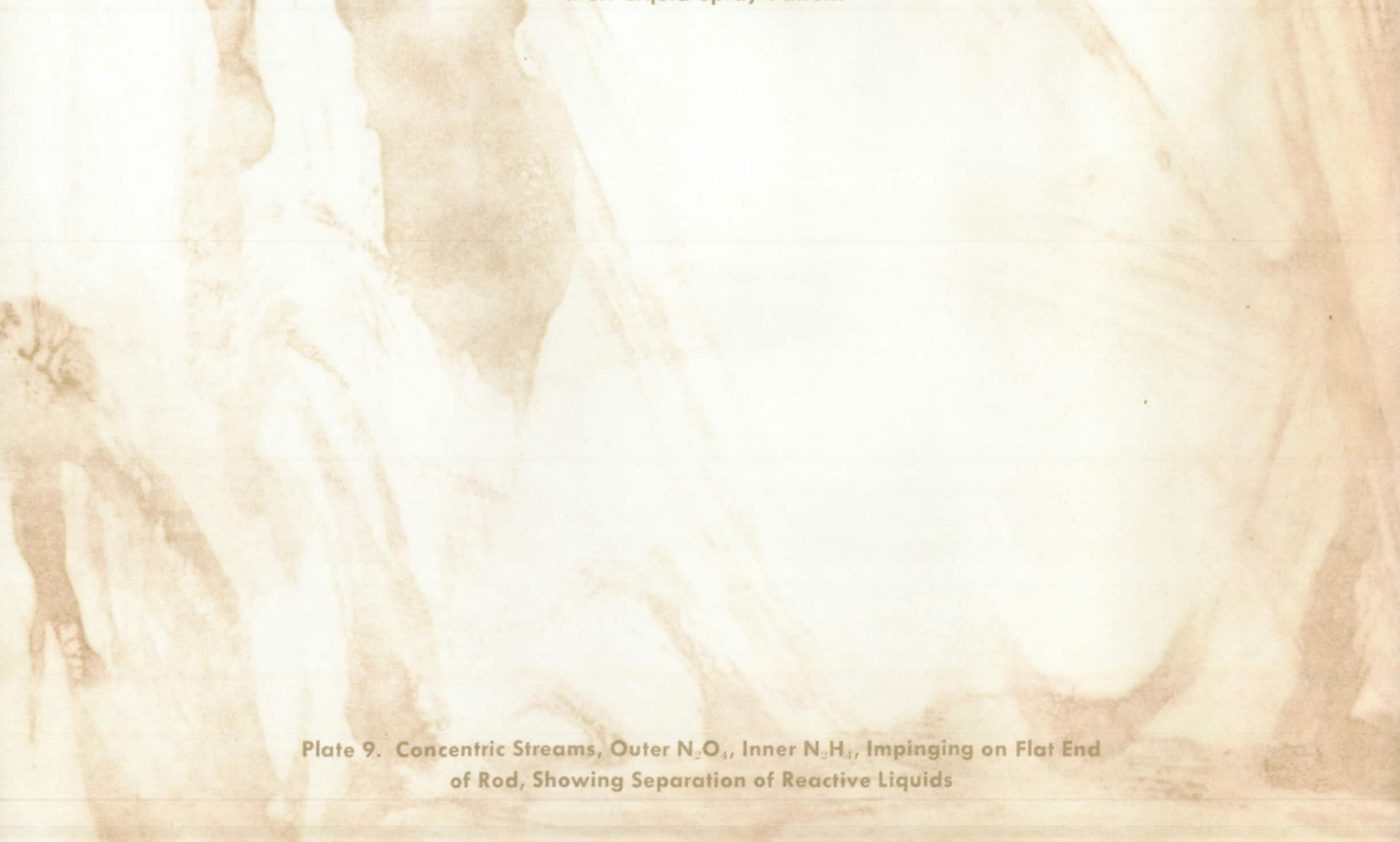

Plate 9. Concentric Streams, Outer $N_2O_4$, Inner $N_2H_4$, Impinging on Flat End of Rod, Showing Separation of Reactive Liquids

Plate 10. $N_2O_4$ Stream Impinging at 180 deg on $N_2H_4$ Stream, Showing Separation

Plate 11. $N_2O_4$ Stream Impinging at 120 deg on $N_2H_4$ Stream, Showing Separation

**Plate 12. $N_2O_4$ Stream Impinging at 45 deg on $N_2H_4$ Stream, Showing Separation**

**Plate 13. View of 80-lb-Thrust Motor Using Impinging Doublet with $N_2O_4$–$N_2H_4$**

**Plate 14. Portion of High-Speed Motion Picture of 80-lb-Thrust Motor Using Doublet Injector with $N_2O_4$–$N_2H_4$, Showing Explosions of Partially Mixed Fuel**

**Plate 15. Schematic Diagram of Injector Showing Impinging-Stream Distribution Characteristics With and Without a Splash Plate, Using $N_2O_4$–$N_2H_4$**

Plate 16. Concentric Tubes Having Knife-Edge Inner Tube, Showing Resulting Stream with Water in Both Center Tube and Annulus

Plate 17. Concentric Tubes Having Knife-Edge Inner Tube, Showing Dispersion and Combustion with SFNA in Annulus and JPX in Center Tube (0.27-in. Retraction)

Plate 18. Concentric Tubes Having Knife-Edge Inner Tube, Showing Near-uniform Vapor Mixture of SFNA–JPX with Resulting Flame Zone (0.35-in. Retraction)

Plate 19. Concentric Tubes Having Knife-Edge Inner Tube, Showing Operation with SFNA–UDMH (Zero Retraction)

Plate 20. Concentric Tubes Having Knife-Edge Inner Tube, Showing Separation of Annular $N_2H_4$ from Center Stream $N_2O_4$ (Zero Retraction)

Plate 21. Concentric Tubes Having Distributor Pin at End of Inner Tube, Using $N_2O_4$–$N_2H_4$

Plate 22. Concentric Tubes of Plate 21 with Injector Face Plate

Plate 23. Concentric-Tube Injector of Plate 22 with 0.15-in.-long Chamber

Plate 24. Concentric-Tube Injector of Plate 22 with 1.0-in.-long Chamber

Plate 25. Concentric-Tube Injector of Plate 22 with Propellants Reversed ($N_2H_4$ in Annulus)

Plate 26. Concentric-Tube Injector of Plate 25 with 0.15-in.-long Chamber

Plate 27. Concentric-Tube Injector of Plate 25 with 1.0-in.-long Chamber

## REFERENCES

1. Elverum, G. W., Jr., and Mason, D. M., *The Effect of Chemical Composition of Fuming Nitric Acid and the Aniline–Furfuryl Alcohol System on Performance and Ignition Delay in Rocket Motors,* Progress Report No. 20-261. Jet Propulsion Laboratory, Pasadena, April 13, 1955 (Confidential).

2. Elverum, G. W., Jr., and Morey, T. F., *A Concentric Premixing Element for Highly Reactive Propellants,* Memorandum No. 30-6. Jet Propulsion Laboratory, Pasadena (to be published).

3. Rupe, J. H., *A Correlation Between the Dynamic Properties of a Pair of Impinging Streams and the Uniformity of Mixture-Ratio Distribution in the Resulting Spray,* Progress Report No. 20-209. Jet Propulsion Laboratory, Pasadena, March 28, 1956.

4. Elverum, G. W., Jr., and Morey, T. F., *Criteria for Optimum Mixture-Ratio Distribution Using Several Types of Impinging-Stream Injector Elements,* Jet Propulsion Laboratory, Pasadena (to be published).

5. Bartz, D. R., "A Simple Equation for Rapid Estimation of Rocket Nozzle Convective Heat Transfer Coefficients," *Jet Propulsion,* 27(1):49-51, January 1957.